Received: 22 October 2025 | Revised: 27 January 2026 | Accepted: 4 March 2026

DOI: 10.1002/rvr2.70045

RESEARCH ARTICLE

River IWHR WILEY

Study of meteorological-hydrological drought propagation under reservoir regulation using a Copula-Bayesian network in the Hanjiang River Basin

Yanping Qu[1,2] | **Cheng Li**[1,2] | **Yachao Zhang**[1,2] | **Siyu Zhao**[1,2,3] | **Tianliang Jiang**[1,2] | **Qinghua Ye**[4,5]

[1]State Key Laboratory of Water Cycle and Water Security, China Institute of Water Resources and Hydropower Research, Beijing, China

[2]Research Center on Flood and Drought Disaster Reduction, China Institute of Water Resources and Hydropower Research, Beijing, China

[3]College of Hydraulic & Environmental Engineering, China Three Gorges University, Yichang, China

[4]Delft University of Technology Faculty of Civil Engineering and Geosciences, Delft, The Netherlands

[5]Deltares, Delft, The Netherlands

Correspondence

Tianliang Jiang, State Key Laboratory of Water Cycle and Water Security, China Institute of Water Resources and Hydropower Research, Beijing 100038, China.
Email: jiangtl@iwhr.com

Funding information

National Key Research and Development Program Funded Project, Grant/Award Number: 2023YFC3006604; Challenge Program of China Institute of Water Resources and Hydropower Research, Grant/Award Number: JZ110145B0112025; Key Research and Development Program of Jiangxi Province, Grant/Award Number: 20232BBG70029-1; Water Conservancy Technology Demonstration Project, Grant/Award Number: SF-202511

Abstract

Reservoir operations play a pivotal role in modifying drought propagation processes, particularly by influencing the transition from meteorological to hydrological drought. This study investigates the drought propagation characteristics in the middle reaches of the Hanjiang River Basin, China, under both natural and observed (reservoir-influenced) conditions. The Standardized Precipitation Evapotranspiration Index and Standardized Streamflow Index were utilized to characterize meteorological and hydrological drought, respectively. The Soil and Water Assessment Tool was employed to reconstruct natural streamflow, providing a baseline for comparison. A nonlinear copula function was applied to model the dependence between meteorological and hydrological drought characteristics, and a Copula-Bayesian network was developed to quantify propagation probabilities. Under the regulation of the Danjiangkou Reservoir, drought propagation characteristics for 1–12-month timescales have shifted markedly: the average propagation time downstream was prolonged from 0.25–0.70 months to 0.94–2.36 months, while the propagation rate declined from 0.83–0.89 to 0.48–0.65, and the sensitivity decreased from 0.83–0.96 to 0.68–0.79. In the natural scenario, the optimal propagation model was based on the Gumbel copula, whereas the observed scenario was best fitted by the Frank copula. The likelihood of hydrological drought increased with the intensity and duration of meteorological drought. However, compared to natural conditions, reservoir regulation significantly delayed the onset and reduced the probability of hydrological drought occurrence. These findings elucidate the nonlinear dynamics of drought propagation and underscore the regulating effect of large-scale reservoirs on downstream hydrological responses.

KEYWORDS

Copula-Bayesian network, Danjiangkou Reservoir, drought propagation, hydrological drought, meteorological drought

1 | INTRODUCTION

Drought, stemming from insufficient precipitation or an imbalance in the water budget, has significant impacts on human activities and ecosystems (Bhardwaj et al., 2020; Wang et al., 2022a; Zhu et al., 2024). Recently, global warming has intensified the frequency of drought and flood events (Chiang et al., 2021; He et al., 2024; Xu et al., 2023). Drought is typically categorized into four types: meteorological, hydrological, agricultural, and socio-economic drought (Wilhite & Glantz, 1985; Zhao et al., 2019). Drought propagation refers to the transition from one type to another (Eltahir & Yeh, 1999; Zhou et al., 2021). In general, meteorological drought marks the initial stage of drought propagation, primarily triggered by prolonged precipitation deficits (Fang et al., 2020; Li et al., 2020; Yuan et al., 2017). Persistent meteorological drought reduces soil moisture and runoff, which can evolve into hydrological drought if water resources are not replenished in a timely manner (Heim, 2002; Xu et al., 2019). As a result, hydrological drought often follows meteorological drought and exerts a more significant impact on socio-economic systems (Espinosa-Tasón et al., 2022; Geng & Shen, 1992; Liu et al., 2023a, 2023b; Wu et al., 2021a).

Hydrological and meteorological droughts exhibit a closely linked response relationship (Ding et al., 2021; Liu et al., 2023c). However, in recent decades, human activities such as reservoir construction, land-use changes, and inter-basin water transfers have increasingly altered the hydrological cycle, directly affecting meteorological-hydrological (M-H) drought propagation (Jehanzaib et al., 2020; Wen et al., 2020). Notably, large reservoirs regulate runoff, thereby modifying the formation and progression of hydrological droughts (Shiau, 2023; Wu et al., 2021b; Xu et al., 2019), with cascading effects on agricultural production, residential water supply, and ecosystems (Chen et al., 2019; Lin et al., 2017; Van Loon et al., 2016). Consequently, investigating M-H drought propagation under reservoir regulation is critical for enhancing drought monitoring, disaster prevention, and mitigation strategies (Wang et al., 2024; Zhang et al., 2023a).

Reservoirs regulate downstream streamflow by storing floodwater and releasing it during dry periods, thereby fulfilling functions such as flood control, water supply, hydropower generation, and navigation (Abdi-Dehkordi et al., 2021; Jain et al., 2023). These reservoir operations substantially reshape the temporal distribution of downstream streamflow, leading to pronounced changes in hydrological drought characteristics and drought propagation mechanisms (Zhang et al., 2022; Zhao et al., 2019). Specifically, they influence the timing, duration, intensity, and frequency of hydrological droughts, thereby altering the propagation pathways from meteorological to hydrological droughts. Large reservoirs often weaken the correlation between meteorological and hydrological droughts, particularly during high-flow periods (Xing et al., 2021), and may even trigger hydrological droughts prior to meteorological ones (Zhang, et al., 2023). For instance, in the Jinjiang River Basin, reservoir operations were found to lower the threshold for drought propagation, intensifying changes in drought duration and severity (Wu et al., 2017). Similarly, Wang et al. (2019) observed that reservoirs increased the frequency of hydrological droughts, characterized by earlier onset, delayed termination, and prolonged duration in response to meteorological droughts. The characteristics of drought propagation also depend on operational purposes; for example, whether a reservoir serves water supply functions affects the magnitude of change in the duration and severity of hydrological droughts, leading to varied propagation impacts (Senbeta et al., 2024). In reservoir networks, downstream reservoirs tend to respond more sharply to early meteorological droughts, showing higher severity, while drought conditions across upstream and downstream areas converge around peak droughts (van Langen et al., 2021). In contrast, Pachorea et al. (2024) found stronger M-H drought correlations upstream, with further weakening downstream under shorter meteorological drought time scales. Overall, the effects of reservoir operations on drought propagation are complex and highly context-dependent across basins and river reaches.

In the study of drought propagation, correlation analysis methods are widely used to determine the propagation time of drought (Ho et al., 2021; Narasimhan & Srinivasan, 2005; Wang et al., 2021). Furthermore, Linear and nonlinear models are often employed to construct the relationship between meteorological and hydrological drought, revealing propagation thresholds (Chen et al., 2020; Huang et al., 2021; Wu et al., 2017). While these studies have significantly advanced research on the propagation relationship between meteorological and hydrological droughts, drought propagation is inherently a probabilistic event (Raposo et al., 2023). Therefore, alternative approaches are required to address this issue. Bayesian networks are widely used for probabilistic analysis in uncertain environments (Hwang & Cho, 2007; Li et al., 2022; Madadgar & Moradkhani, 2014), while copula functions have significant advantages in establishing joint analyses among multiple variables (Ma et al., 2013; Poonia et al., 2021). The combination of Bayesian networks and Copula functions offers a novel approach for analyzing propagation probabilities between different types of droughts (Jiang et al., 2024; Romeo José et al., 2006; Wu et al., 2023).

The Danjiangkou (DJK) Reservoir, a strategic water control project in the Hanjiang River Basin (HRB), began impoundment in November 1967. Extensive research has documented the spatiotemporal characteristics of meteorological and hydrological droughts in the HRB (Jin et al., 2024; Liu et al., 2015; Liu et al., 2018; Wang et al., 2022b). Previous studies have demonstrated that DJK Reservoir operations have substantially altered the HRB's hydrological regime and ecosystem dynamics (Wang et al., 2015; Zhang et al., 2018; Zhou, et al., 2024). Although the dominant role of anthropogenic factors has been established (Li et al., 2024), the specific nonlinear mechanisms by which the DJK Reservoir reshapes M-H drought propagation remain unclear. Given its substantial regulation capacity and the distinct shift in hydrological regimes it has induced, the DJK Reservoir provides a representative case for examining how reservoir operations decouple hydrological droughts from meteorological drivers. Consequently, this study employs the DJK Reservoir as a case study to validate the applicability of the proposed Copula-Bayesian network in capturing these complex interactions. Crucially, this study moves beyond confirming that "reservoirs reduce drought" to revealing how they alter the probabilistic structure of drought propagation—specifically by decoupling the tail dependence of extreme events, as evidenced by the shift from Gumbel to Frank Copula. Specifically, by evaluating drought propagation patterns under natural and observed scenarios, this study aims to:

(a) develop a model to characterize drought propagation with and without reservoir influence; (b) quantify the impact of the DJK Reservoir on downstream drought propagation characteristics; and (c) evaluate the alteration of the DJK Reservoir on drought propagation probability. The findings not only contribute to the methodologies for assessing drought propagation under reservoir regulation but also provide valuable insights into drought propagation mechanisms and early warning systems (Figure 1).

2 | STUDY AREA AND DATA

2.1 | Study area

The HRB, the longest tributary of the Yangtze River, spans a length of 1577 km and covers an area of approximately 159,000 km². It is situated between 106°12′–114°20′ E longitude and 30°08′–34°11′ N latitude. Located within the subtropical monsoon zone, the HRB is characterized by significant topographical diversity and spatiotemporal heterogeneity in precipitation distribution. Consequently, the region frequently experiences extended periods of drought (Liu et al., 2018; Zhang et al., 2023b). For instance, in June 2017, persistent high temperatures over the HRB led to rapid drought development, with drought severity reaching severe to extreme levels in some regions. Similarly, in May 2022, a sharp decrease in rainfall affected 2381 hectares of cropland. The DJK Reservoir is located at the confluence of the Hanjiang and Danjiang Rivers. The reservoir features a normal pool level of 170 m, a dead water level of 150 m, and a flood-control level of 160 m, with a total storage capacity of 31.95 billion m³. Under normal operating conditions, water is released in early May to lower the water level to accommodate the flood season, followed by staged impoundment from mid-August to early October (Ouyang et al., 2018). To ensure water supply efficiency, reservoir outflow is curtailed based on tiered water level thresholds (Figure 2). Specifically, when water levels drop to Supply Reduction Level 1 and Level 2, outflows are reduced by a maximum of 15% and 20%, respectively. Therefore, the reservoir plays a crucial role in regulating runoff, significantly influencing hydrological processes in the middle and lower reaches of the basin. The Huangjiagang (HJG) station is located 6 km downstream from the DJK Reservoir, and its streamflow is significantly affected by the operation of the reservoir (Wang et al., 2023a). The Shayang (SY) Station marks the boundary between the middle and lower reaches of the Hanjiang River (Lu et al., 2018).

2.2 | Data

The monthly precipitation data from 1968 to 2022 were sourced from the 1 km resolution monthly precipitation and average temperature dataset for China, provided by the National Tibetan Plateau Data Center (http://data.tpdc.ac.cn). Monthly observed streamflow data from 1968 to 2022 for the HJG and SY stations, together with inflow, outflow, and water level data for the DJK Reservoir, were obtained from the Changjiang Water Resources Commission. The natural streamflow data for the HJG and SY hydrological stations from 1968 to 2022 were reconstructed using the Soil and Water Assessment Tool (SWAT) hydrological model. The simulated results were validated against other natural runoff data (CRND v1.0; Miao & Gou, 2022), confirming their reliability (Li et al., 2024) (Figure 3).

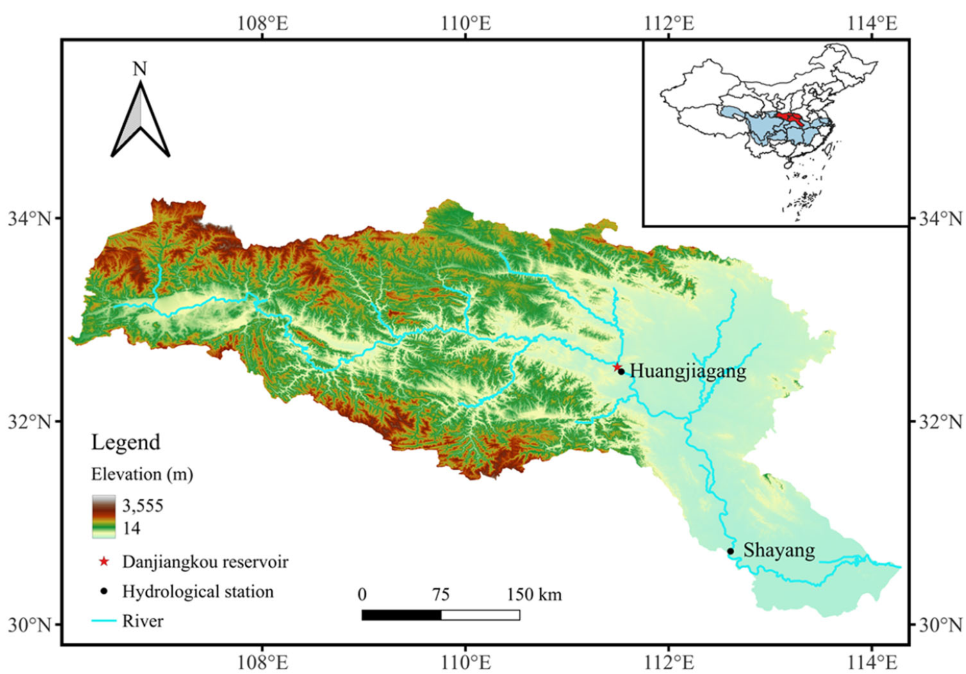

FIGURE 1 Distribution of reservoir and hydrological stations in the HRB.

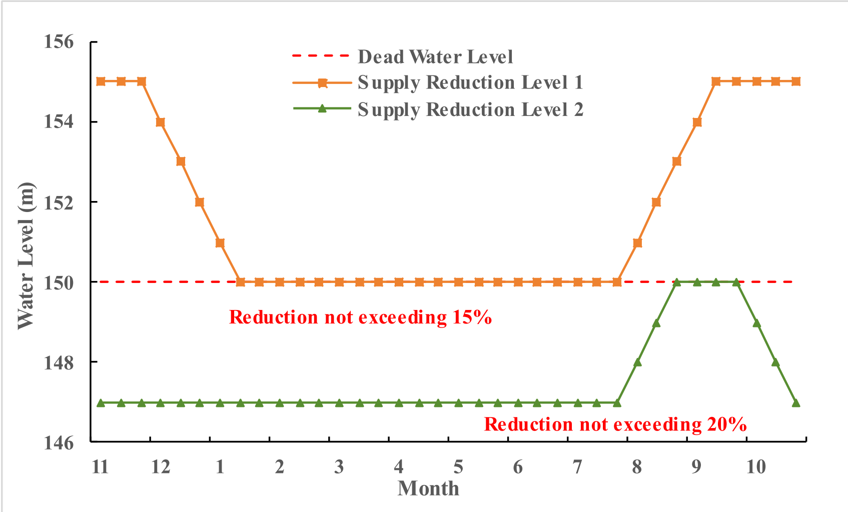

FIGURE 2 DJK Reservoir operation rules schematic under drought conditions.

3 | METHODOLOGY

3.1 | Drought propagation events identification

3.1.1 | Natural streamflow reconstruction based on the SWAT model

The SWAT model, characterized by its robust physical mechanisms, demonstrates strong capability in simulating streamflow under diverse climate scenarios and anthropogenic influences (Arnold et al., 1998). This model has been widely employed in hydrological drought attribution studies (Prasanchum et al., 2022; Wang et al., 2023b). The SWAT model simulates the hydrological cycle based on the water balance equation (Mtibaa & Asano, 2022):

$$SW_t = SW_0 + \sum_{i=1}^{t}(R_{\text{day}} - Q_{\text{surf}} - E_a - W_{\text{seep}} - Q_{gw}), \quad (1)$$

where SW_t represents the final soil water content; SW_0 represents the initial soil water content; R_{day} is the precipitation; Q_{surf} denotes the surface runoff; E_a represents the evapotranspiration; W_{seep} is the amount of water percolating into the vadose zone from the soil profile; and Q_{gw} denotes the return flow.

During the baseline period (1961–1967), observed streamflow data were treated as representing natural hydrological conditions. This period represents the only continuous record of natural streamflow observations available prior to the construction of the DJK Reservoir and was therefore used for SWAT model calibration (1961–1965) and validation (1966–1967). Figure 4 presents the simulated versus observed monthly streamflow at four monitoring stations. Model performance metrics for both calibration and validation periods met acceptable thresholds ($\text{NSE} > 0.7$, $R^2 > 0.8$, $\text{logNSE} > 0.7$, and $|\text{PBIAS}| < 20\%$); detailed calculation methods for these metrics can be found in Li et al. (2024). These results demonstrate the model's effectiveness in simulating natural streamflow regimes in the HRB. While flood peak simulations showed some limitations due to inherent model uncertainties, this did not affect hydrological drought analyses since drought processes primarily occur during dry periods. Previous research (Jiang et al., 2019) confirmed that accurate dry-period simulations were sufficient for reliable drought assessment, with flood period deviations having a negligible impact on drought characterization.

3.1.2 | Drought index calculation

The Standardized Precipitation Evapotranspiration Index (SPEI) (Vicente-Serrano et al., 2010) and the Standardized Streamflow Index (SSI) (Vicente-Serrano et al., 2012) were utilized to characterize meteorological and hydrological droughts, respectively. Both SSI and SPEI can be calculated at various time scales, for example, 1 month, 3 months, 6 months, and 12 months. Short time scales are mainly related to soil water content and river discharge in headwater areas, while medium time scales are associated with reservoir storages and discharge in the medium course of rivers, and long time scales reflect variations in groundwater storage (Vicente-Serrano et al., 2010). Due to the lagged response inherent in drought propagation, persistent meteorological droughts are more likely to develop into hydrological droughts (Van Loon, 2015). Seasonal drought indices are generally more suitable for identifying continuous drought events (Chen et al., 2020). Therefore, considering the influence of seasonality, the 3-month time scale was selected for calculating SSI and SPEI (Wu et al., 2016; Wu et al., 2017). The SSI was derived from streamflow data, and the corresponding SPEI was computed using the average precipitation and temperature of the catchment area. Detailed calculation procedures are described in Vicente-Serrano et al. (2010) and Vicente-Serrano et al. (2012).

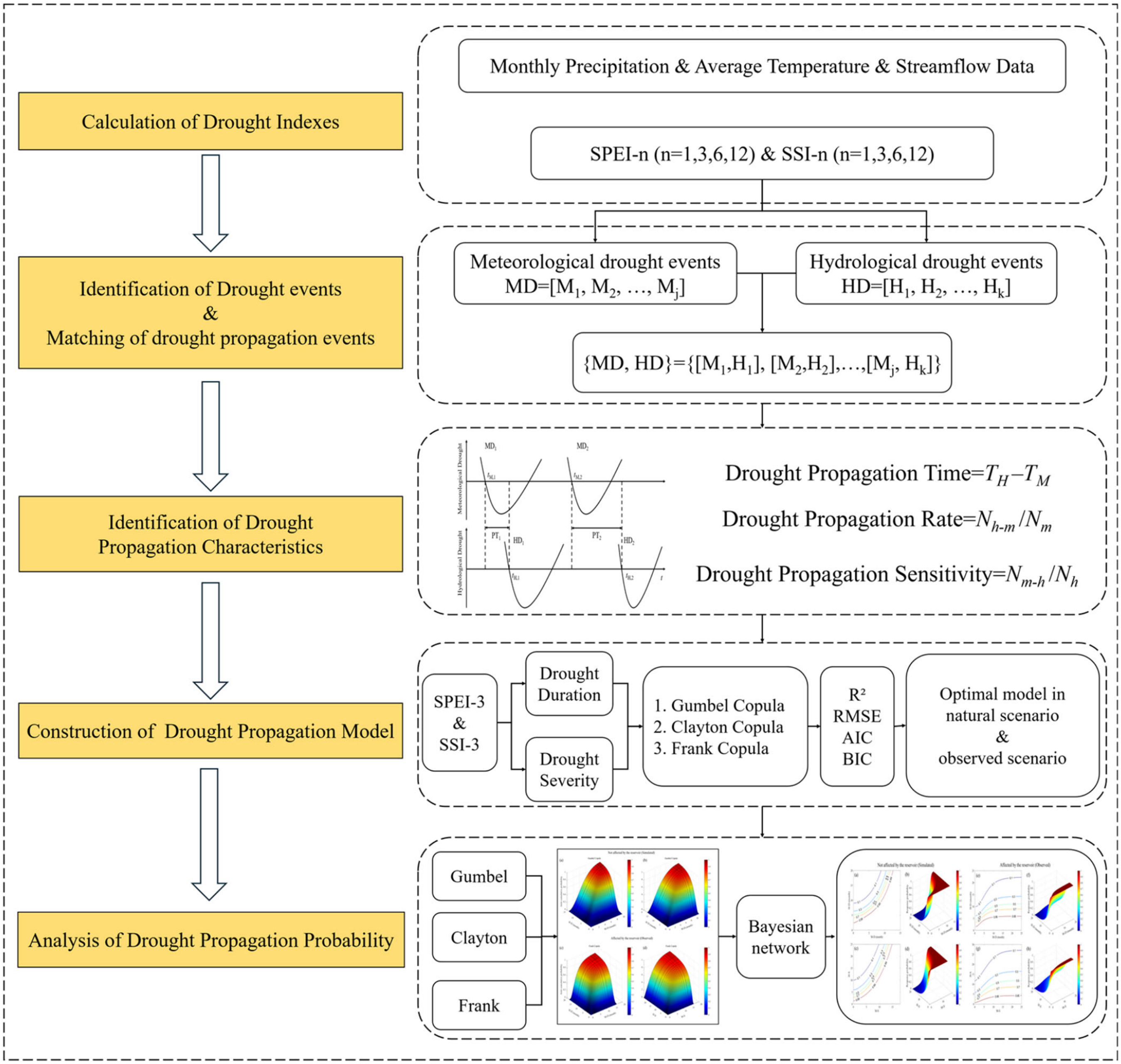

FIGURE 3 The framework for assessing propagation from meteorological to hydrological drought under the influence of Danjiangkou Reservoir.

3.1.3 | Drought identification and drought propagation events matching

Meteorological and hydrological drought events were identified using the SPEI-3 and SSI-3 drought indices based on the three-threshold run theory (Figure 5, $X_0 = 0$, $X_1 = -0.5$, $X_2 = -1$) (Wang et al., 2024; Yevjevich, 1967). The duration (D) and severity (S) of meteorological (M) and hydrological (H) droughts were extracted, and then M-H drought propagation events were matched. This study used the following criteria for matching drought propagation:

1. Temporal Overlap Matching
   If the occurrence period of a meteorological drought overlaps with that of a hydrological drought, the hydrological drought is attributed to the meteorological drought. These events are considered paired (e.g., Event 1 in Figure 6).
2. Temporal Threshold Matching
   When the onset of a hydrological drought occurs after the termination of its corresponding meteorological drought (e.g., Event 2 in Figure 6), a predefined time threshold ($PT_{\text{threshold}}$) is applied. Propagation is confirmed, and events are matched if and only if the observed lag time (PT) satisfies $PT < PT_{\text{threshold}}$. Otherwise, no causal linkage is established. An overextended $PT_{\text{threshold}}$ could lead to spurious drought propagation attribution due to increasing interference from non-meteorological

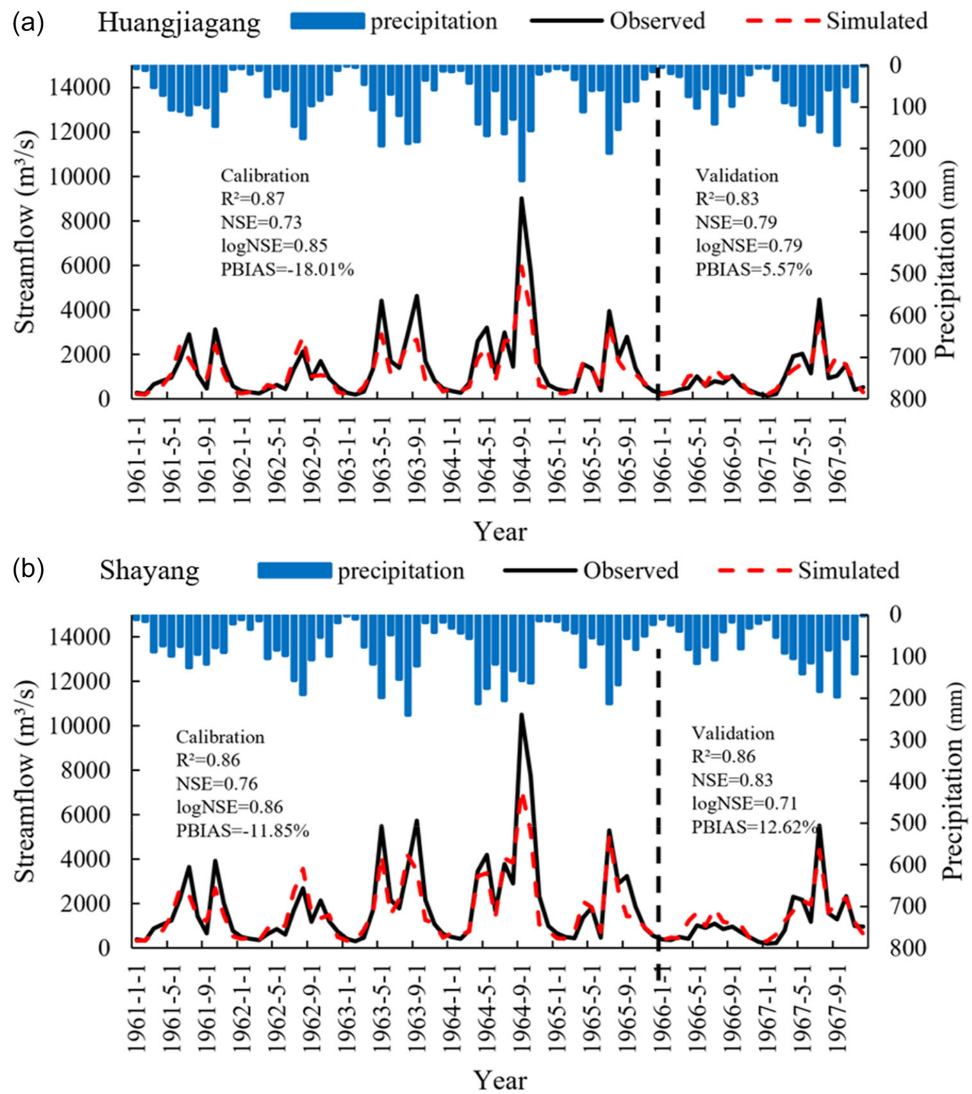

FIGURE 4 Streamflow simulation from 1961 to 1967.

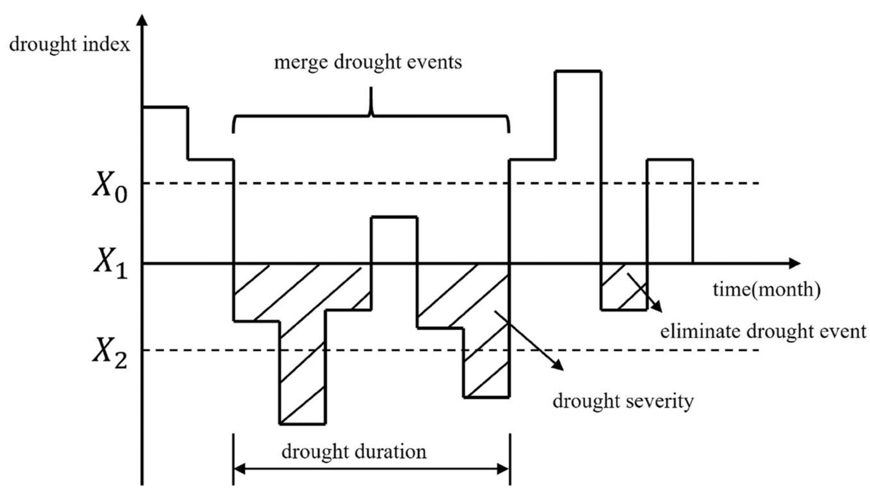

FIGURE 5 Schematic diagram of the three threshold run theory.

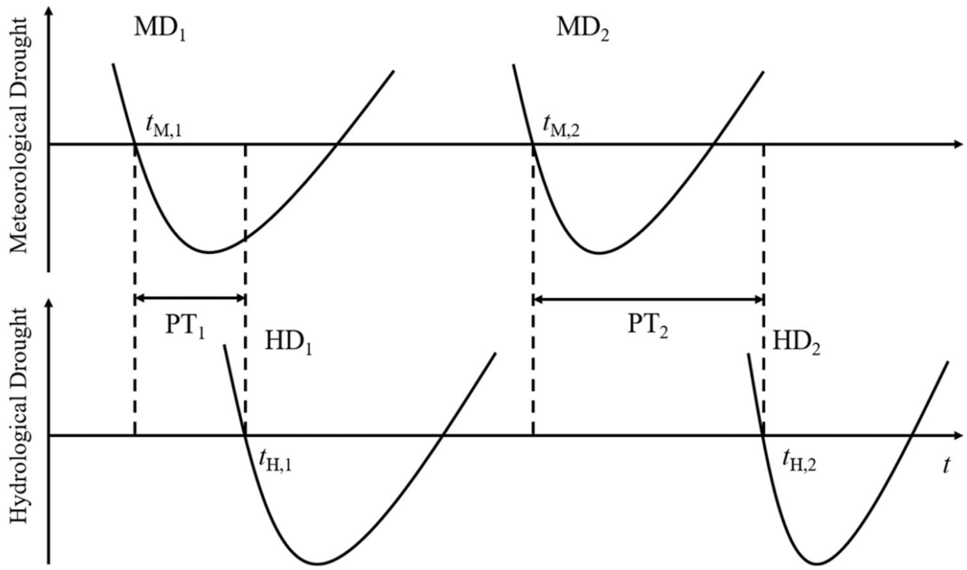

FIGURE 6 Schematic diagram of matching drought propagation events.

factors. In humid regions, precipitation is the primary source of streamflow, and the response time of hydrological drought to meteorological drought is relatively short (Zhou, et al., 2024). The HRB is located in a humid to semi-humid climate region and exhibits a relatively rapid hydrological response. Previous research indicated that the propagation time from meteorological to hydrological drought onset in the HRB during 1990–2015 ranged from 2.7 to 3.2 months, while that for drought peaks ranged from 1.3 to 3 months (Zhang, et al., 2023). Therefore, in this study, the $PT_{\text{threshold}}$ is set to 3 months.

3. Anomalous Event Exclusion

   Hydrological droughts exhibiting prolonged duration and high severity are excluded from meteorological drought attribution when paired with short-duration, low-severity meteorological droughts, as such disparities suggest alternative driving mechanisms. The drought propagation time (PT) is quantified via Equation (2):

$$PT = t_{H,n} - t_{M,n}, \tag{2}$$

where, $t_{H,n}$ is the onset time of the n-th hydrological drought event, and $t_{M,n}$ is the onset time of the n-th meteorological drought event.

3.1.4 | Drought propagation rate and sensitivity

Due to the complexity of the propagation process, meteorological drought does not invariably lead to hydrological drought. Conversely, one meteorological drought may trigger several hydrological droughts, or several meteorological droughts may jointly result in one hydrological drought. Therefore, this study characterizes drought propagation according to the drought propagation rate and sensitivity (Guo et al., 2020). The drought propagation rate and sensitivity are calculated as shown in Equations (3) and (4):

$$T_{r1} = \frac{N_{h-m}}{N_m}, \tag{3}$$

$$T_{r2} = \frac{N_{m-h}}{N_h}, \tag{4}$$

where T_{r1} and T_{r2} represent drought propagation rate and sensitivity, respectively; N_m represents the total number of meteorological droughts; N_h represents the total number of hydrological droughts; and $N_{h\text{-}m}$ represents the number of meteorological droughts that lead to hydrological droughts; $N_{m\text{-}h}$ represents the number of hydrological droughts triggered by meteorological droughts.

3.2 | Construction of a nonlinear propagation model based on Copula function

Following Hao et al. (2016), conditional probabilities based on Copula functions can be used to establish nonlinear relationships between variables and for probability prediction. Drawing on this framework, this study establishes a nonlinear response model between the meteorological characteristic variable X and the hydrological drought characteristic variable Y, and then derives the conditional probability distribution of the response of the hydrological drought characteristic variable to the meteorological drought characteristic variable. By setting $F_X(x)$ and $F_Y(y)$ represent the marginal distribution functions of X and Y, respectively. Let $u = F_X(x)$ and $v = F_Y(y)$, the joint distribution function and probability density function of X and Y are expressed in Equation (5) and Equation (6) respectively:

$$F(x, y) = C[F_X(x), F_Y(y)] = C(u, v), \quad (5)$$

$$f(x, y) = c(u, v) \cdot f_X(x) \cdot f_Y(y), \quad (6)$$

where C denotes the Copula function, $f_X(x)$ and $f_Y(y)$ are the marginal probability density functions of X and Y. Given $X = x$, the conditional probability density distribution function for the occurrence of variable Y, can be derived as Equations (7) and (8):

$$\begin{aligned} F_{Y|X}(y) &= P(Y \leq y/X = x) = \frac{\partial F(x, y)/\partial x}{dF_X(x)/dx} \\ &= \frac{\partial C(u, v)}{\partial u}, \end{aligned} \quad (7)$$

$$\begin{aligned} f_{Y|X}(y) &= \frac{f(x, y)}{f_X(x)} = \frac{c(u, v) \cdot f_X(x) \cdot f_Y(y)}{f_X(x)} \\ &= c(u, v) \cdot f_Y(y). \end{aligned} \quad (8)$$

The maximum value of the conditional probability density function, obtained when $df_{Y|X}(y)/dy = 0$ corresponds to the predicted value of Y. The conditional probability, cumulative distribution function, and the probability density function of variable Y are illustrated in Figure 7.

3.3 | Copula-Bayesian-based drought propagation probability model

While conditional probabilities derived from Copula functions facilitate nonlinear modeling and prediction (Hao et al., 2016), integrating them with Bayesian network models enhances probabilistic inference. Seven common marginal distribution functions (Normal, Gamma (Gam), Weibull (Wb), Lognormal (LogN), Logistic, Loglogistic (LogL), and Extreme Value) and three Copula joint distribution functions were used to fit the duration and severity of droughts at the HJG and SY stations. The optimal fitting functions were selected based on the Kolmogorov–Smirnov (K–S) test, Akaike Information Criterion (AIC), Bayesian Information Criterion (BIC), and Root Mean Square Error (RMSE). The two-dimensional Copula function is formulated as shown in Equation (9):

$$C(m, n) = C[f_A(a), f_B(b)], \quad (9)$$

where a and b are variables; f_A and f_B are the cumulative marginal distribution functions of a and b; C (m, n) is the Copula joint distribution function.

The Bayesian network can effectively address uncertainty problems by combining conditional probability methods to estimate the correlation between variables (Sattar et al., 2019). This study adopts a first-order Bayesian network model:

$$P(A_2/A_1) = \frac{P(A_1/A_2)}{P(A_1)}. \quad (10)$$

The result obtained from the Copula joint distribution function is the probability that one variable is less than a and the other variable is less than b. When combined with a Bayesian network, the result becomes the probability that the dependent variable is greater than b given that the independent variable is greater than a. This probabilistic output is beneficial for estimating the propagation probability of different hydrological drought scenarios when meteorological drought occurs. The expression derived from the combination of the copula joint distribution function and Bayesian network model can be represented as Equation (11) (Guo et al., 2020):

$$\begin{aligned} P(B \geq b|A \geq a) &= \frac{P(A \geq a, B \geq b)}{P(A \geq a)} \\ &= \frac{1 - f_A(a) - f_B(b) + C[f_A(a), f_B(b)]}{1 - f_A(a)} \\ &= 1 - \frac{f_B(b) - C[f_A(a), f_B(b)]}{1 - f_A(a)}. \end{aligned} \quad (11)$$

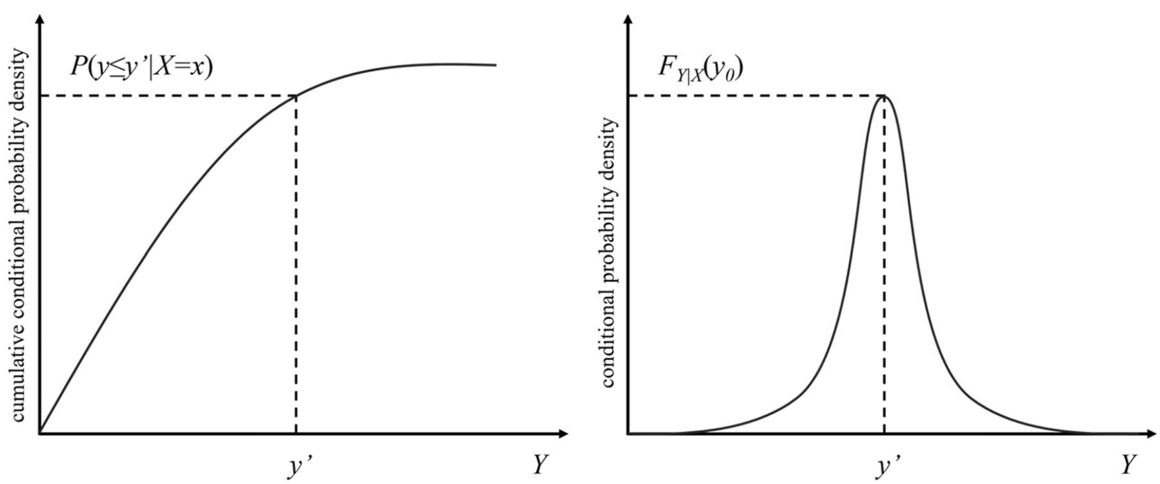

FIGURE 7 Conditional probability, cumulative distribution function, and probability density function for variable Y.

The specific modeling steps are as follows:

1. Correlation Analysis: First, the correlation between the hydro-meteorological characteristic variables was assessed. Only when the correlation between the two constructed variables reaches a significant level can they be jointly constructed. Previous studies have demonstrated a significant synergistic effect between the duration and severity of droughts, which jointly reflect the intensity of meteorological flash droughts (Sreeparvathy & Srinivas, 2022). Furthermore, several studies have employed these as marginal variables (Wu et al., 2017; Yang et al., 2024). Therefore, this study selects duration and severity as marginal variables.
2. Marginal Distribution Fitting: Next, the optimal marginal distribution functions for individual drought characteristic variables were identified.
3. Copula Parameter Estimation: Based on the preferred marginal distributions for each drought characteristic variable, three common Archimedean Copula functions (Gumbel, Clayton, and Frank) were selected. The parameters of the Copula joint distribution functions were estimated using the maximum likelihood method.
4. Joint Distribution Selection: Then, the optimal distribution functions for the joint variables (M-D, H-D, M-S, and H-S) were established (M and H represent meteorological drought and hydrological drought, respectively; D and S represent duration and severity, respectively).
5. Probability Calculation: Finally, the marginal distribution functions for each variable and the joint distribution function for the joint variables were incorporated into the Bayesian network probability model to calculate the propagation probability.

4 | RESULTS

4.1 | Changes in drought propagation characteristics influenced by the DJK reservoir

The average propagation time of M-H drought at the HJG Station and SY Station at 1-, 3-, 6-, and 12-month time scales under natural and observed scenarios is illustrated in Figure 8. For the HJG Station, the average propagation time under the natural scenario from 1968 to 2022 ranged from 0.25 to 0.65 months across the time scales of 1, 3, 6, and 12 months. Under the observed scenario, the average drought propagation time increased markedly to 0.94–2.36 months. Similarly, at the SY Station, the average propagation time under the natural scenario was 0.30–0.70 months. Under the observed scenario, the average duration of drought propagation increased to 1.14–2.36 months. With increasing timescales, the average propagation time lengthens, and compared to the natural scenario, the average drought propagation time is significantly extended in the observed scenario.

The drought propagation rate and sensitivity of the HJG Station and SY Station at various scales are shown in Table 1. The drought propagation rates of the HJG Station from 1968 to 2022 under the natural scenario were 0.86–0.88; those at the SY Station on time scales of 1, 3, 6, and 12 months were 0.83–0.89. Under the natural scenario, the drought propagation rate remains relatively stable as the time scale increases. In contrast, under the observed scenario, the drought propagation rates at HJG Station dropped to 0.54–0.65; and at the were 0.48–0.65, respectively. Compared to the natural scenario, the drought propagation rate has significantly decreased in the

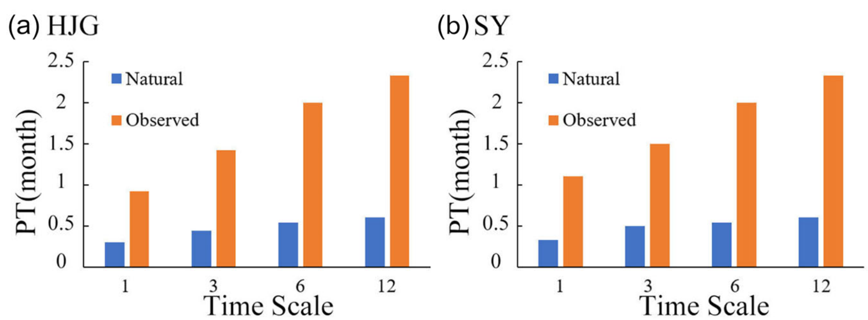

FIGURE 8 Drought propagation time of HJG and SY station in natural and observed scenarios.

TABLE 1 Drought propagation rate and sensitivity.

Station	Period		1-month Natural	Observed	3-month Natural	Observed	6-month Natural	Observed	12-month Natural	Observed
HJG	1968–2022	T_{r1}	0.86	0.54	0.87	0.60	0.88	0.60	0.88	0.65
		T_{r2}	0.94	0.68	0.92	0.71	0.95	0.70	0.95	0.69
SY	1968–2022	T_{r1}	0.83	0.48	0.89	0.57	0.88	0.48	0.88	0.65
		T_{r2}	0.96	0.79	0.96	0.79	0.95	0.76	0.83	0.73

observed scenario, with a more pronounced decrease at shorter timescales.

Under the natural scenario, the drought sensitivity of the HJG Station was 0.92–0.95; while that of the SY Station 0.83–0.96. Under the observed scenario, the drought sensitivity of the HJG Station decreased to 0.68–0.71; and that of the SY Station was 0.73–0.79. As the time scale increases, the sensitivity to drought does not change significantly. Compared to the natural scenario, the sensitivity to drought decreases significantly in the observed scenario, with the HJG Station experiencing a greater decrease than the SY Station. The decrease in the propagation rate of drought indicates a reduction in the proportion of meteorological drought propagating to hydrological drought under the observed scenario. The decrease in drought sensitivity indicates an increase in the proportion of hydrological drought driven by human activities.

4.2 | Construction of drought propagation models based on Copula function

This section employs drought indices at a 3-month time scale to extract drought characteristics and develop the drought propagation model. The correlation between drought characteristics at the two stations was assessed, and the results are presented in Table 2. A high correlation was observed between the meteorological and hydrological drought characteristics at both stations. Therefore, the duration and severity of meteorological and hydrological drought were selected as marginal variables for constructing a joint distribution model.

To identify the optimal drought propagation model, the drought propagation events were divided into calibration and validation subsets (Wu et al., 2017). The optimal propagation model was selected based on validation results. Previous studies indicate that the goodness-of-fit of a function is related to the ratio of calibration and validation subsets, and a ratio of 2:1 is optimal (Shao, 1997). Therefore, the first two-thirds of the events were used for model calibration, while the remaining events were used for validation.

TABLE 2 The correlation coefficients between meteorological and hydrological drought characteristic variables. (** indicates significance at $\alpha = 0.01$).

Station	Characteristics	Scenario	Pearson	Kendall	Spearman
HJG	M-D, H-D	Natural	0.9624**	0.8785**	0.9421**
		Observed	0.9096**	0.7390**	0.8668**
	M-S, H-S	Natural	0.9628**	0.7492**	0.9138**
		Observed	0.8496**	0.6043**	0.7836**
SY	M-D, H-D	Natural	0.9732**	0.8914**	0.9446**
		Observed	0.9313**	0.8797**	0.9622**
	M-S, H-S	Natural	0.9671**	0.8083**	0.9337**
		Observed	0.8853**	0.6667**	0.8523**

Five probability distribution functions, namely Normal, Gamma (Gam), Weibull (Wb), Lognormal (LogN) and Logistic, and Loglogistic (LogL) distributions, were tested to fit the drought duration and severity of meteorological and hydrological drought events in the calibration subset. The selection of optimal marginal distribution was primarily based on the Kolmogorov–Smirnov (K–S) test. Here, h and P denote the K–S test statistics. The h statistic is a binary decision indicator (0 or 1) for the hypothesis test. When h is 0, it indicates that the K–S test has passed the 5% significance level, meaning the distribution model provides a good fit to the observed drought duration and severity data. The p value represents the probability value; a larger p value indicates a higher probability that the empirical distribution and theoretical distribution are consistent. All distributions passed the K–S test ($h = 0$).

As detailed in Table 3, in the natural scenario, the optimal distributions of meteorological drought duration (MD), meteorological drought severity (MS), hydrological drought duration (HD), and hydrological drought severity (HS) at the HJG station were the Logistic, LogN, LogN, and LogN distributions; at the SY station, they were the LogL, LogL, LogL, and Gam distributions. In the observed scenario, the optimal distributions of MD, MS, HD, and HS at the HJG station were the LogN, LogN, LogL, and LogN distributions; while those at the SY station were the LogN, LogL, LogN, and LogL distributions.

Three Archimedean Copula functions (Gumbel, Clayton, and Frank) were evaluated. RMSE, AIC, and BIC were used as goodness-of-fit metrics. The goodness of fit for the three Copula functions is presented in Table 4. In the natural scenario, the optimal joint copula distribution for drought characteristics was the Gumbel Copula, while in the observed scenario, it was the Frank Copula.

Using the established Copula functions, the nonlinear propagation model was applied to simulate the hydrological drought duration and severity values based on meteorological drought duration and severity in the validation set. The optimal drought propagation model is presented in Table 5 and Figure 9. As the duration and severity of meteorological drought increased, so did the corresponding hydrological drought characteristics. From the perspective of drought duration, the curve for the natural scenario lay above that of the observed scenario at the SY station. The HJG station also exhibited this pattern during meteorological droughts lasting less than 9 months. This indicates that under the same meteorological drought conditions, the observed hydrological drought duration is shorter. The drought severity fitted curve for the natural scenario was also positioned above the observed scenario, indicating that reservoir operations have mitigated drought propagation. However, in the observed scenario, one extreme drought propagation event occurred, causing the tail of the curve to surpass the natural scenario. This indicated that reservoir operation mitigated short-duration and

TABLE 3 Optimal marginal distribution of drought characteristics.

				K–S test statistical value (*p*-value)						
Scenario	**Drought type**	**Station**	**Drought characteristic**	**Normal**	**Gam**	**Wb**	**LogN**	**Logistic**	**LogL**	**Optimal distribution**
Natural	M	HJG	Duration	0.27	0.38	0.42	0.40	**0.54**	0.26	Logistic
			Severity	0.30	0.70	0.67	**0.86**	0.54	0.77	LogN
		SY	Duration	0.08	0.34	0.25	0.46	0.29	**0.66**	LogL
			Severity	0.12	0.66	0.43	0.88	0.50	**0.95**	LogL
	H	HJG	Duration	0.09	0.44	0.20	**0.52**	0.46	0.42	LogN
			Severity	0.14	0.30	0.32	**0.59**	0.28	0.51	LogN
		SY	Duration	0.11	0.45	0.26	0.74	0.47	**0.76**	LogL
			Severity	0.40	**0.97**	0.89	0.95	0.69	0.94	Gam
Observed	M	HJG	Duration	0.21	0.44	0.43	**0.72**	0.33	0.64	LogN
			Severity	0.49	0.53	0.53	**0.73**	0.57	0.60	LogN
		SY	Duration	0.23	0.51	0.51	**0.74**	0.39	0.69	LogN
			Severity	0.13	0.50	0.51	0.86	0.44	**0.91**	LogL
	H	HJG	Duration	0.22	0.42	0.41	0.65	0.42	**0.74**	LogL
			Severity	0.23	0.46	0.45	**0.70**	0.36	0.64	LogN
		SY	Duration	0.39	0.54	0.56	**0.78**	0.54	0.74	LogN
			Severity	0.15	0.48	0.61	0.80	0.25	**0.88**	LogL

Note: Bold values denote the optimal marginal distribution.

low-severity drought propagation events. Conversely, when encountering multiple prolonged meteorological droughts in a row, multiple hydrological drought events under the natural scenario were merged by reservoir regulation, resulting in a prolonged duration and increased severity of a single hydrological drought event.

4.3 | Drought propagation probability analysis

To quantify the propagation probability of hydrological drought characteristics corresponding to meteorological drought characteristics, the entire dataset of drought propagation events was utilized for model construction. The optimal fitting functions were selected based on the K–S test results, as shown in Table 6. Specifically, the optimal marginal distribution for M-D at the HJG station was the Wb for the distribution, the natural scenario, and the LogN distribution for the observed scenario, while H-D was best fitted by the LogL distribution. The optimal marginal distribution for M-S and H-S were Wb and LogN, respectively. At the SY station, the natural and observed scenarios favored the LogL and LogN distributions for M-D and H-D, respectively. The optimal marginal distribution for M-S in the natural scenario was LogN, and for the observed scenario, it was the LogL distribution. The optimal distribution for H-S was the LogL distribution.

The goodness of fit was assessed using RMSE, AIC, and BIC, with the results presented in Table 7. The joint probability distribution of drought characteristic variables is presented in Figures 10 and 11. The optimal joint copula function for drought duration and severity in the natural scenario was the Gumbel copula. In contrast, the optimal joint copula function in the observed scenario was the Frank copula. Generally, an increase in M-D (M-S) resulted in a higher joint cumulative probability. When M-D (M-S) was low, the joint cumulative probability rose rapidly with an increase in M-D (M-S). Conversely, when M-D (M-S) was high, the rate of increase in the joint cumulative probability slowed significantly. Overall, while holding hydrological drought duration (H-D) or severity (H-S) constant, the joint cumulative probability increased with an increase in M-D (M-S), though the rate of increase attenuated over time.

The propagation probabilities between meteorological and hydrological drought characteristic variables are shown in Figures 12 and 13. The slope of the propagation probability curve indicates the rate of change in the propagation probability, while the spacing between contours reflects the degree of variability in propagation probability. It can be observed that the propagation probabilities of hydrological drought duration and severity increase with the increase of meteorological drought duration and severity. Notably, the rate of increase of M-H drought propagation probability contours is steeper in the natural scenario compared to the observed scenario. As a result, meteorological droughts were more likely to induce severe hydrological droughts without the influence of reservoirs.

TABLE 4 Goodness of fit test and parameters of the copula function.

Scenario	Station	Drought characteristics	Copula	Parameter	AIC	BIC	RMSE
Natural	HJG	M-D, H-D	**Gumbel**	**4.2998**	**−143.94**	**−142.41**	**0.1169**
			Clayton	4.0005	−134.17	−132.64	0.1350
			Frank	17.1601	−142.01	−140.48	0.1203
		M-S, H-S	**Gumbel**	**4.1349**	**−212.44**	**−210.91**	**0.0427**
			Clayton	1.7928	−185.04	−183.51	0.0639
			Frank	13.1450	−209.18	−207.66	0.0448
	SY	M-D, H-D	**Gumbel**	**5.7220**	**−163.15**	**−161.63**	**0.0881**
			Clayton	5.8589	−156.61	−155.09	0.0970
			Frank	17.0228	−160.60	−159.08	0.0915
		M-S, H-S	**Gumbel**	**4.2245**	**−205.43**	**−203.90**	**0.0473**
			Clayton	2.2516	−169.89	−168.36	0.0798
			Frank	13.4289	−204.38	−202.85	0.0481
Observed	HJG	M-D, H-D	Gumbel	3.1507	−72.40	−71.56	0.1121
			Clayton	1.8863	−65.96	−65.13	0.1355
			Frank	**11.2847**	**−74.55**	**−73.72**	**0.1052**
		M-S, H-S	Gumbel	3.2470	−83.08	−82.24	0.0819
			Clayton	1.3050	−74.22	−73.39	0.1062
			Frank	**9.6702**	**−83.34**	**−82.51**	**0.0812**
	SY	M-D, H-D	Gumbel	4.5788	−71.12	−70.29	0.1164
			Clayton	2.9692	−67.51	−66.67	0.1295
			Frank	**21.6757**	**−74.13**	**−73.30**	**0.1065**
		M-S, H-S	Gumbel	4.2245	−204.38	−202.85	0.0481
			Clayton	2.2516	−169.89	−168.36	0.0798
			Frank	**13.4289**	−205.43	−203.90	**0.0473**

TABLE 5 Optimal meteorological-hydrological propagation model.

Scenario	Station	Drought characteristics	Propagation model	R^2	RMSE	AIC	BIC
Natural	HJG	Duration	Gumbel Copula	0.86	1.22	9.61	10.38
		Severity	Gumbel Copula	0.90	1.08	5.53	6.30
	SY	Duration	Gumbel Copula	0.93	0.75	−6.39	−5.56
		Severity	Gumbel Copula	0.95	0.86	−1.93	−1.10
Observed	HJG	Duration	Frank Copula	0.95	1.21	6.13	6.21
		Severity	Frank Copula	0.98	0.71	−2.23	−2.15
	SY	Duration	Frank Copula	0.96	1.17	5.58	5.66
		Severity	Frank Copula	0.98	1.24	6.53	6.61

In the observed scenario, when meteorological drought duration and severity were small, the propagation probability of hydrological drought changed rapidly. However, with the increase in meteorological drought characteristics, the rate of increase in the propagation probability of hydrological drought diminished, eventually reaching stability. The propagation probability achieved a relative stability when the meteorological drought characteristic variables exceeded a specific threshold. Taking the HJG station as an example, when the meteorological drought

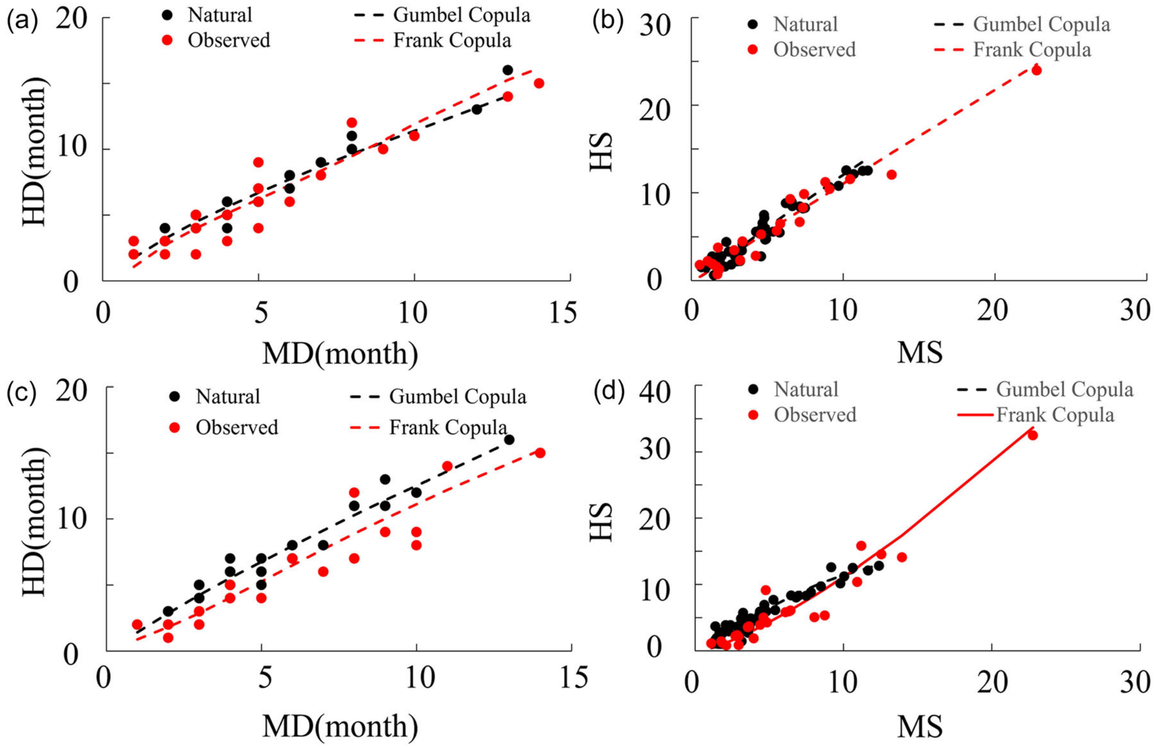

FIGURE 9 Best-fit drought propagation models in the HJG (a, b) and SY (c, d) stations.

TABLE 6 Optimal fitting function and K–S test for marginal distribution of drought characteristics.

		HJG		SY	
Drought type	**Scenario**	**D**	**S**	**D**	**S**
Meteorological	Natural	Wb	Wb	LogL	LogN
	Observed	LogN	Wb	LogN	LogL
Hydrological	Natural	LogL	LogN	LogL	LogL
	Observed	LogL	LogN	LogN	LogL

duration lasted over 10 months, the probability of the hydrological drought duration lasting more than 10 months remained around 50%. When the hydrological drought duration exceeded 15 months, the probability remained below 30% regardless of the meteorological drought duration. In the natural scenario, when the M-D exceeded 5, 10, and 15 months, the respective probabilities of H-D duration exceeding 15 months were 4.21%, 60.82%, and 99.99%. With M-S severity at 5, 10, and 15, the corresponding probabilities of H-S severity exceeding 15 were 8.71%, 65.81%, and 99.99%, respectively. In contrast, in the observed scenario, for meteorological drought durations of 5, 10, and 15 months, the probabilities of H-D duration exceeding 15 months were only 8.73%, 19.46%, and 24.19%, respectively. With M-S severity exceeding 5, 10, and 15, the corresponding probabilities of H-S severity exceeding 15 were 13.37%, 25.81%, and 32.62%, respectively.

5 | DISCUSSION

5.1 | Efficacy of the Copula-Bayesian network in drought propagation analysis

In the study of drought propagation, linear and nonlinear function models are often used to construct the relationship between meteorological and hydrological drought characteristics such as drought duration and severity (Huang et al., 2021; Wu et al., 2017; Yang et al., 2024). Although linear models provide a straightforward structure for characterizing drought propagation (Chen et al., 2020), their assumption of linearity does not align with the complex nonlinear characteristics observed in practice, especially given that drought propagation involves multiple mechanisms with complex and dynamic relationships. For instance, the correlation between meteorological and hydrological drought often changes with time and environmental conditions. Studies indicate that the relationship between meteorological and hydrological drought has undergone significant changes under the influence of human activities (Huang et al., 2021; Wu et al., 2024; Ye et al., 2016). In particular, the operation of large reservoirs has significant impacts on hydrological processes. Linear models are conceptually too simplistic to fully capture these complexities, especially given their inability to reveal changes caused by human activities (Van Loon & Laaha, 2015; Van Loon et al., 2016). In contrast, the Copula method enhances drought propagation assessment by providing probabilistic quantification, which effectively captures nonlinear relationships between

TABLE 7 Evaluation of the goodness of fit of copula function.

Station	Variables	Scenario	Copula	Parameter	AIC	BIC	RMSE
HJG	M-D&H-D	Natural	**Gumbel**	**3.9056**	**−228.7105**	**−226.7985**	**0.0995**
			Clayton	4.1012	−213.9088	−211.9968	0.1154
			Frank	16.5068	−220.9743	−219.0623	0.1076
		Observed	Gumbel	2.9295	−118.4435	−117.2246	0.0899
			Clayton	1.8402	−108.7304	−107.5116	0.1092
			Frank	**9.3513**	**−119.9001**	**−118.6812**	**0.0873**
	M-S&H-S	Natural	**Gumbel**	**3.8848**	**−320.8010**	**−318.8890**	**0.0396**
			Clayton	2.9557	−288.8526	−286.9405	0.0546
			Frank	15.1231	−309.4178	−307.5058	0.0444
		Observed	Gumbel	2.1071	−132.3210	−131.1021	0.0681
			Clayton	1.5876	−122.6684	−121.4495	0.0826
			Frank	**7.2248**	**−136.9669**	**−135.7480**	**0.0621**
SY	M-D&H-D	Natural	**Gumbel**	**5.4115**	**−241.6177**	**−239.6858**	**0.0918**
			Clayton	6.3159	−237.5311	−235.5993	0.0955
			Frank	17.1784	−240.1238	−238.1920	0.0931
		Observed	Gumbel	4.4339	−119.8558	−118.6369	0.0874
			Clayton	2.6850	−111.6201	−110.4013	0.1031
			Frank	**19.3822**	**−122.5501**	**−121.3312**	**0.0828**
	M-S&H-S	Natural	**Gumbel**	**4.2193**	**−336.2871**	**−334.3553**	**0.0363**
			Clayton	2.3837	−268.3387	−266.4068	0.0706
			Frank	15.0802	−332.0889	−330.1570	0.0378
		Observed	Gumbel	2.8034	−154.3726	−153.1538	0.0438
			Clayton	2.1457	−142.6559	−141.4370	0.0554
			Frank	**9.6581**	**−157.9732**	**−156.7544**	**0.0408**

meteorological and hydrological drought indices (Van de Vyver & Van den Bergh, 2018; Wu et al., 2022). Copula models allow researchers to accommodate marginal distributions specific to the distinct characteristics of these indices. For example, the Gumbel copula is more suitable for natural scenarios, as it exhibits upper-tail dependence, indicating that extreme meteorological droughts are likely to coincide with extreme hydrological droughts. In contrast, the Frank copula performs better under observed scenarios because it lacks tail dependence, suggesting that reservoir regulation weakens the linkage between these extreme drought events. Rather than focusing on fitting a deterministic response curve, a key innovation of this work is the integration of the Copula function with a Bayesian network (the Copula–Bayesian method). This method extends the analysis from simple "one-to-one" relationships to the domain of conditional probabilities. Specifically, in addition to investigating the correspondence between meteorological drought of a given severity level (e.g., grade X) and the associated severity of hydrological drought (Figure 9), we further quantified the likelihood that a meteorological drought of grade X would propagate and lead to a hydrological drought of at least severity Y (Figures 12 and 13). This shift from deterministic to probabilistic analysis provides deeper insights and more practical decision-making support for basin-scale drought risk assessment, early warning, and water resources management.

Using this framework, our results demonstrate that the operation of the DJK Reservoir in the HRB effectively reshapes the propagation patterns from meteorological to hydrological drought. Specifically, reservoir regulation substantially weakens the propagation linkage, with both propagation rate and sensitivity being markedly lower in the observed scenario than in the natural scenario, particularly at shorter timescales. This indicates that more hydrological droughts are linked to human regulation rather than meteorological drivers. For instance, Senbeta et al. (2024) found that about 70% of meteorological droughts in the Pilica River basin evolved into hydrological

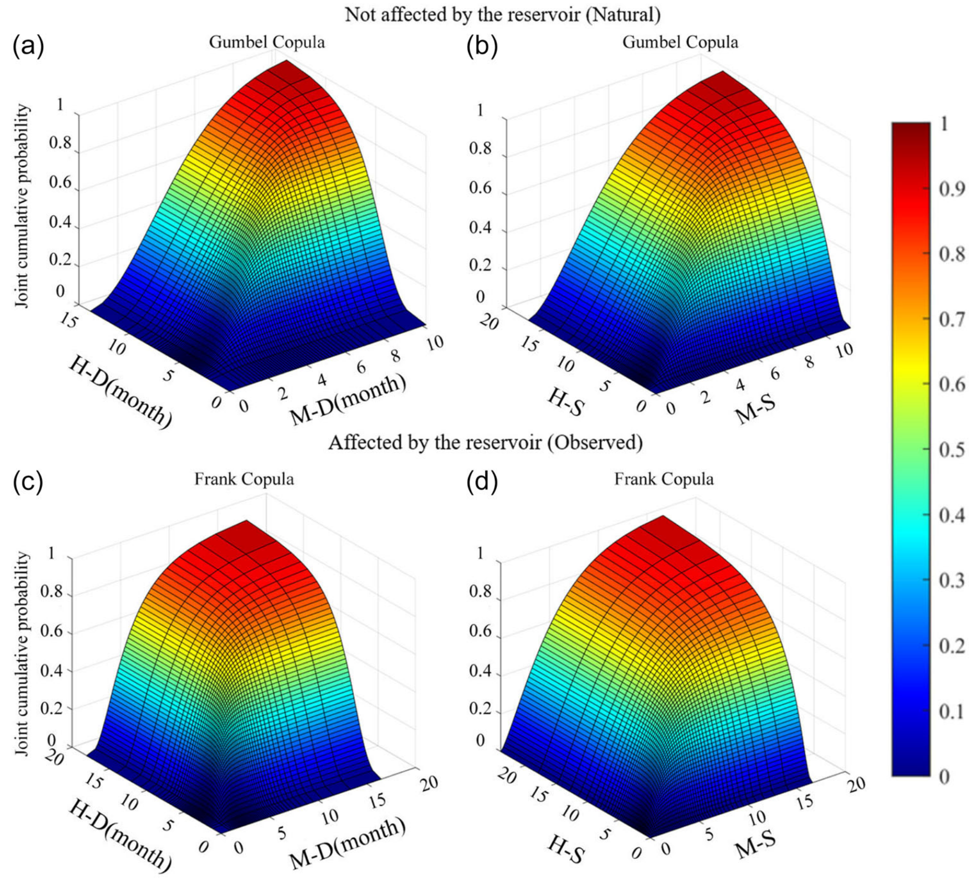

FIGURE 10 Joint probability distribution of M-H drought characteristic at HJG.

droughts, with ~10% induced by anthropogenic activities. Reservoir regulation effectively mitigates short-term, low-intensity droughts: under similar meteorological conditions, hydrological droughts in the observed scenario lasted longer but were less severe. This is consistent with Wang et al. (2019), who reported more frequent and prolonged droughts under reservoir regulation in the Luanhe River basin, and Wu et al. (2021b), who showed that large reservoirs reduce drought frequency, duration, and severity by storing floodwater and releasing it in dry periods. Likewise, Pachore et al. (2024) observed that drought propagation in reservoir-affected reaches of the Tapi River increased from ~4 to 6 months, aligning with our results. Our analysis further highlights the nonlinear impacts of reservoir operation: without reservoirs, meteorological droughts are more likely to trigger severe hydrological droughts, whereas under reservoir influence, the increase in propagation probability slows with increasing meteorological drought intensity and eventually stabilizes beyond a threshold.

5.2 | The physical mechanism of reservoir regulation on hydrological drought

The Danjiangkou (DJK) Reservoir significantly alters drought propagation dynamics by prolonging propagation times and reducing both propagation rates and sensitivity. The underlying physical mechanism for this regulation is the reservoir's "store-and-release" operation, which redistributes streamflow seasonally—storing water during wet seasons and augmenting flow during dry periods. Figure 14 provides a concrete and quantitative example of this regulatory mechanism in action during 2014, a representative year characterized by typical seasonal drought events (Zhang et al., 2023b). The period from mid-April to mid-November clearly illustrates a major water storage phase. During this time, the reservoir's water level rose steadily from a low of approximately 136.5 m in mid-April to a peak of about 160.7 m in mid-November, indicating a substantial increase in stored water volume.

This storage operation had two key effects. First, during the relatively dry period from April to early September, the natural inflow into the reservoir was low and fluctuated, often staying below 2000 m³/s. However, the reservoir maintained a stable and consistent outflow (red line) and downstream HJG runoff (yellow area) at around 500 m³/s. By limiting reservoir releases, this operation maintained a stable and slowly rising reservoir water level, while the stable outflow buffered downstream basic water demands and ecosystems against the immediate impacts of meteorological drought. Second, the reservoir demonstrated its capacity for flood peak attenuation during the large autumn flood in mid-September, when inflow spiked to over 12,000 m³/s. Instead of passing this flood downstream,

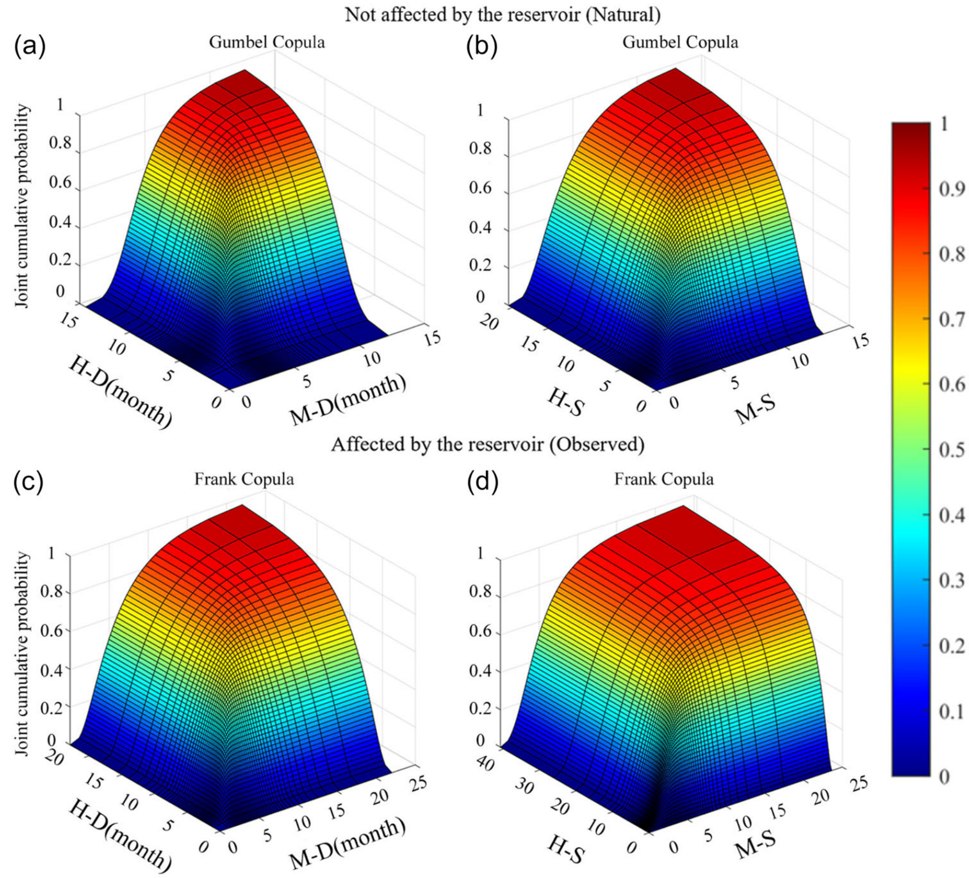

FIGURE 11 Joint probability distribution of M-H drought characteristic at SY.

the reservoir absorbed the peak, with outflow remaining steady at a small fraction of the inflow, around 500 m^3/s. This captured floodwater contributed directly to the sharp rise in water level observed in September and October.

This "store-and-release" strategy, clearly quantified by the 2014 data, is the physical process responsible for the statistically observed delay and mitigation of hydrological droughts. By absorbing both low-flow variability and high-flow peaks, the reservoir disconnects the immediate link between meteorological precipitation deficits and downstream streamflow, which explains the longer propagation times and lower propagation probabilities quantified in our results. While other minor water conservancy projects exist in the middle reaches, their daily regulation capacity has a negligible impact on annual and monthly runoff modulation compared to the large-scale DJK Reservoir.

5.3 | Limitations and future development

Due to the impoundment of the DJK Reservoir starting in November 1967 and the lack of early hydrological data in the HRB, this study calibrated the SWAT model using natural observed streamflow from two hydrological stations in the basin during the period 1961–1965, and validated the SWAT model with data from 1966 to 1967. This period represents the only continuous record of natural streamflow observations available prior to the construction of the DJK Reservoir and was therefore used for model calibration. While it is acknowledged that the relatively short calibration period may pose challenges for parameterization and increase parametric uncertainty, previous studies have demonstrated that SWAT can reasonably reconstruct long-term natural streamflow variability in the HRB under data-limited conditions (Li et al., 2024), which provides support for this study. Such uncertainty mainly manifests in the simulation of flood peaks, while streamflow during dry seasons and drought periods is less influenced, allowing drought conditions to be reliably captured (Jiang et al., 2019). Furthermore, it should be noted that the SWAT model here is primarily used to reconstruct long-term natural streamflow as a baseline scenario for comparative drought propagation analysis, rather than for high-precision simulation of absolute streamflow magnitude. Consequently, the key conclusions of this study are based on relative differences and drought propagation characteristics, which are less sensitive to absolute simulation errors. Future studies may further improve streamflow reconstruction by incorporating longer-term and multi-station natural streamflow sequences to enhance the accuracy of streamflow simulations.

This study developed a nonlinear model based on the copula function to describe the propagation between meteorological and hydrological droughts in the HRB and to

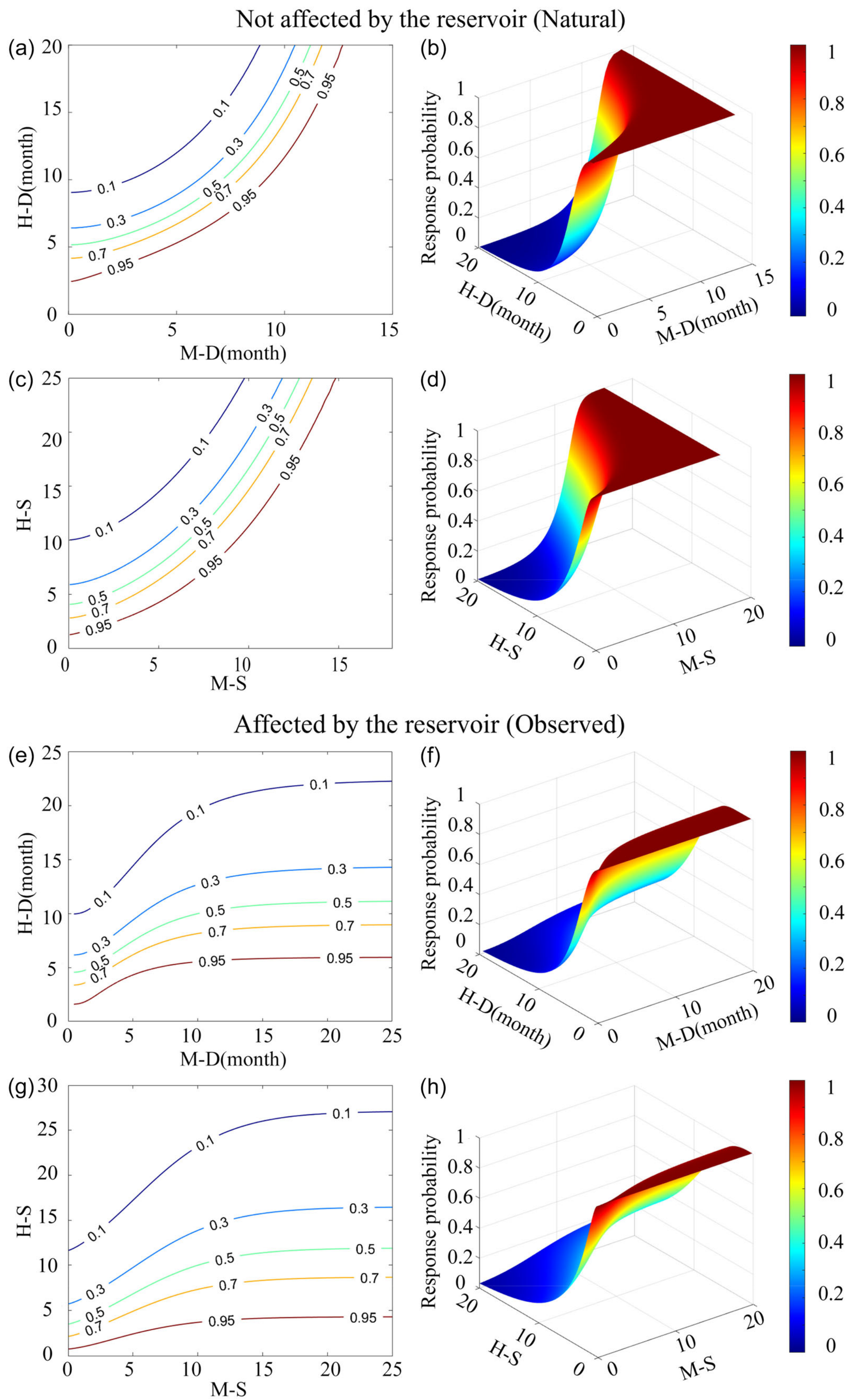

FIGURE 12 M-H drought propagation probability at HJG station.

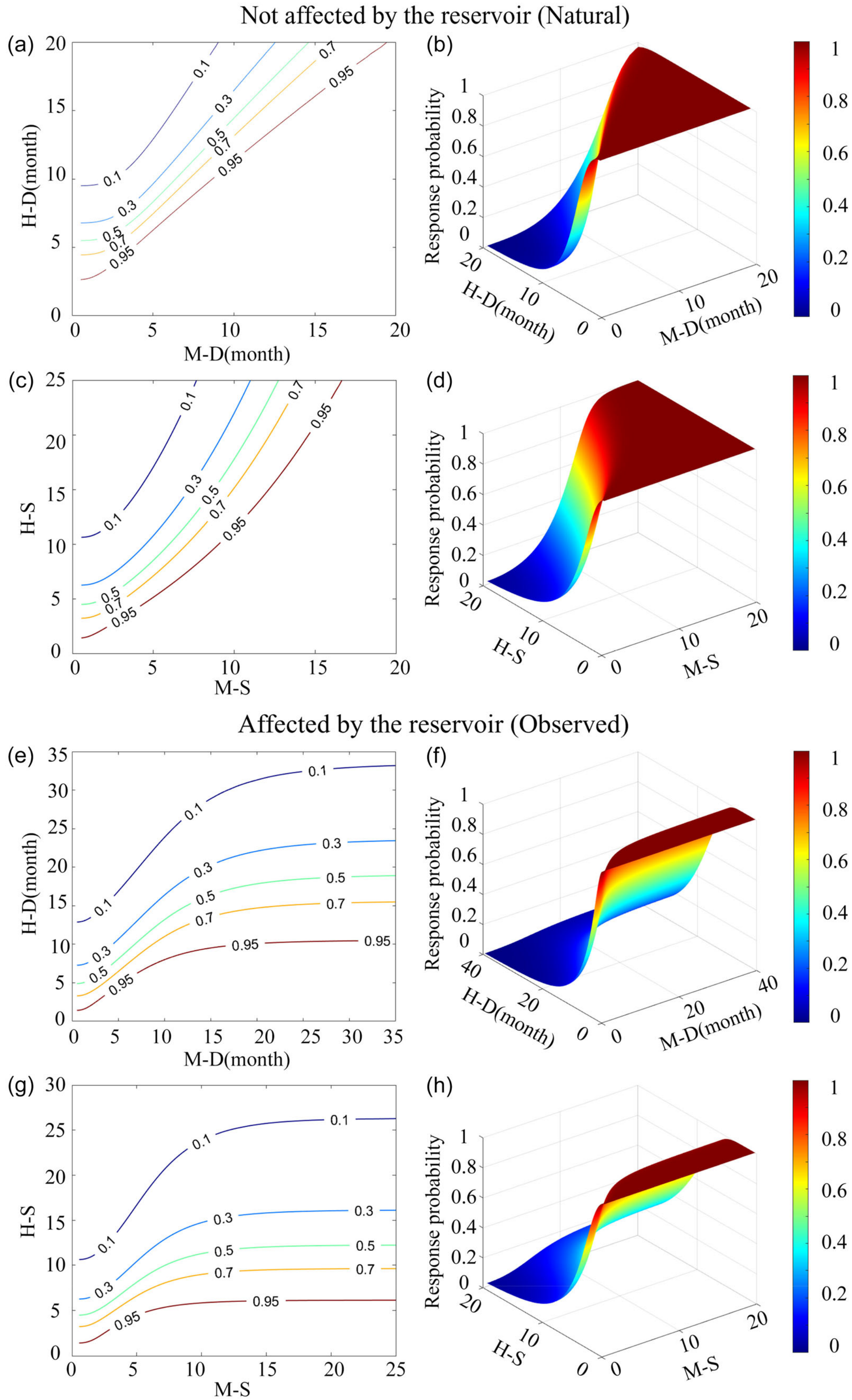

FIGURE 13 M-H drought propagation probability at SY station.

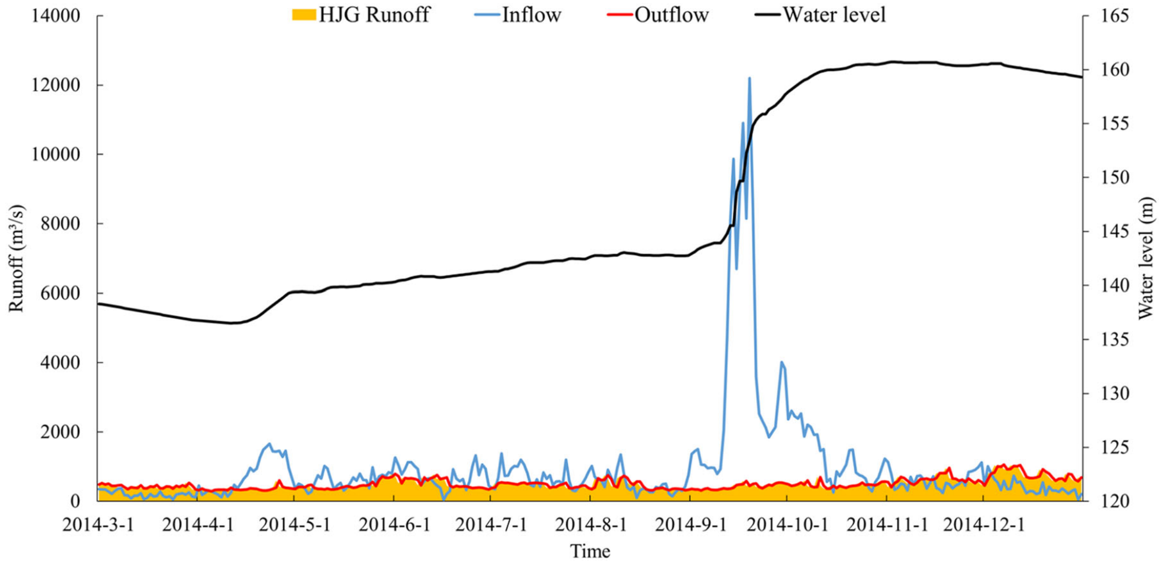

FIGURE 14 Time variation of daily average runoff at HJG Station and daily inflow and outflow of DJK Reservoir.

analyze the impact of the DJK Reservoir. The Copula function, combined with a Bayesian network probability model, was utilized to establish the propagation probability characteristic curves for meteorological and hydrological drought characteristics. The analysis of the propagation probability curves revealed notable differences in hydrological drought responses under reservoir regulation. Hydrological droughts responded more rapidly to meteorological droughts without reservoir influence. However, under the influence of the reservoir, the propagation speed slowed, and the probability of extreme droughts triggered by meteorological droughts decreased significantly. These findings are consistent with those reported by Leitman et al. (2016), Wu et al. (2018), and Wen et al. (2011). Additional operational guidelines for the reservoir could further mitigate downstream hydrological drought duration and severity.

However, this study acknowledged the influence of other human activities but did not explicitly address the potential limitations or biases that might be introduced into the research conclusions. The analysis was confined to qualitative descriptions, lacking a concrete mechanistic explanation or support from existing empirical findings regarding non-reservoir factors. Despite the effectiveness of Copula-Bayesian-based models, this study did not quantitatively analyze other human activity effects, such as agricultural irrigation withdrawal, urban water consumption, or inter-basin water transfers, which might significantly influence drought propagation. In addition, it is necessary to investigate anthropogenic factors and climate change impacts on drought propagation in more detail. Future studies should quantify the contributions of dam operations, urbanization, and irrigation to drought propagation and examine the effects of future climate scenarios using downscaled climate model outputs. In future research, it is necessary to comprehensively consider the combined impact of human activities and climate change.

6 | CONCLUSION

This study utilized a Copula-Bayesian Network framework to quantify the non-linear alteration of drought propagation by the Danjiangkou Reservoir, moving beyond simple correlation analysis to reveal specific probabilistic thresholds. The key findings are summarized as follows:

1. The reservoir significantly delays and decouples the M-H link. Our results indicate that the average propagation time extended from 0.45 to 1.44 months (at the 3-month scale), while drought sensitivity dropped from 0.92 to 0.71. This implies that under reservoir regulation, the hydrological system has shifted from a climate-sensitive regime to a buffered regime where nearly 40% of meteorological droughts fail to trigger hydrological events.
2. The Copula-Bayesian model demonstrated its value by identifying a "probability ceiling" for drought propagation. Unlike the natural scenario, where extreme meteorological droughts (duration >15 months) led to hydrological droughts with 99.99% certainty, reservoir regulation stabilizes this propagation probability at approximately 24%. This finding confirms that the reservoir acts as a probabilistic barrier, effectively truncating off the "tail dependence" of extreme events.

The optimal dependence structure shifted from the Gumbel Copula (natural) to the Frank Copula (observed). This structural change indicates that the reservoir eliminates the high correlation between extreme events found in nature. Although the reservoir effectively mitigates peak severity, its "store-and-release" mechanism introduces a trade-off by merging multiple short-term deficits into prolonged hydrological drought events.

In summary, this study demonstrates that the DJK Reservoir does not merely reduce drought but fundamentally alters the propagation mechanism from a linear, high-probability response to a non-linear, probability-capped system. The proposed probabilistic framework can provide quantitative references for basin-scale drought risk assessment and early warning in similar river basins.

ACKNOWLEDGMENTS

We thank everyone who helped during the manuscript writing. This study was financially supported by the National Key Research and Development Program Funded Project (2023YFC3006604), Challenge Program of China Institute of Water Resources and Hydropower Research (JZ110145B0112025), Key Research and Development Program of Jiangxi Province (20232BBG70029-1), and Water Conservancy Technology Demonstration Project (SF-202511).

DATA AVAILABILITY STATEMENT

The data that support the findings of this study are available from the corresponding author upon reasonable request.

ETHICS STATEMENT

The authors declare that they have no known competing financial interests or personal relationships that could have appeared to influence the work reported in this paper.

ORCID

Yanping Qu https://orcid.org/0000-0002-0532-8617
Yachao Zhang https://orcid.org/0009-0004-7657-1675

REFERENCES

Abdi-Dehkordi, M., Bozorg-Haddad, O., Salavitabar, A., Mohammad-Azari, S., & Goharian, E. (2021). Development of flood mitigation strategies toward sustainable development. *Natural Hazards*, *108*(3), 2543–2567.

Arnold, J. G., Srinivasan, R., Muttiah, R. S., & Williams, J. R. (1998). Large area hydrologic modeling and assessment. Part I: Model development. *JAWRA Journal of the American Water Resources Association*, *34*(1), 73–89.

Bhardwaj, K., Shah, D., Aadhar, S., & Mishra, V. (2020). Propagation of meteorological to hydrological droughts in India. *Journal of Geophysical Research: Atmospheres*, *125*(22), e2020JD033455.

Chen, N., Li, R., Zhang, X., Yang, C., Wang, X., Zeng, L., Tang, S., Wang, W., Li, D., & Niyogi, D. (2020). Drought propagation in Northern China Plain: A comparative analysis of GLDAS and MERRA-2 datasets. *Journal of Hydrology*, *588*, 125026.

Chen, X., Li, F., Li, J., & Feng, P. (2019). Three-dimensional identification of hydrological drought and multivariate drought risk probability assessment in the Luanhe River basin, China. *Theoretical and Applied Climatology*, *137*(3–4), 3055–3076.

Chiang, F., Mazdiyasni, O., & AghaKouchak, A. (2021). Evidence of anthropogenic impacts on global drought frequency, duration, and intensity. *Nature Communications*, *12*(1), 2754.

Ding, Y., Xu, J., Wang, X., Cai, H., Zhou, Z., Sun, Y., & Shi, H. (2021). Propagation of meteorological to hydrological drought for different climate regions in China. *Journal of Environmental Management*, *283*, 111980.

Eltahir, E. A. B., & Yeh, P. J.-F. (1999). On the asymmetric response of aquifer water level to floods and droughts in Illinois. *Water Resources Research*, *35*(4), 1199–1217.

Espinosa-Tasón, J., Berbel, J., Gutiérrez-Martín, C., & Musolino, D. A. (2022). Socioeconomic impact of 2005–2008 drought in Andalusian agriculture. *Science of the Total Environment*, *826*, 154148.

Fang, W., Huang, S., Huang, Q., Huang, G., Wang, H., Leng, G., & Wang, L. (2020). Identifying drought propagation by simultaneously considering linear and nonlinear dependence in the WEI RIVER basin of the Loess Plateau, China. *Journal of Hydrology*, *591*, 125287.

Geng, H., & Shen, B. (1992). Definition and significance of hydrological drought. *Arid Region Agricultural Research*, *10*(4), 91–94.

Guo, Y., Huang, S., Huang, Q., Leng, G., Fang, W., Wang, L., & Wang, H. (2020). Propagation thresholds of meteorological drought for triggering hydrological drought at various levels. *Science of the Total Environment*, *712*, 136502.

Hao, Z., Hao, F., Singh, V. P., Sun, A. Y., & Xia, Y. (2016). Probabilistic prediction of hydrologic drought using a conditional probability approach based on the meta-Gaussian model. *Journal of Hydrology*, *542*, 772–780.

He, N., Yin, J., Slater, L. J., Liu, R., Kang, S., Liu, P., Liu, D., & Xiong, L. (2024). Global terrestrial drought and its projected socioeconomic implications under different warming targets. *Science of the Total Environment*, *946*, 174292.

Heim, R. R. (2002). A review of twentieth-century drought indices used in the United States. *Bulletin of the American Meteorological Society*, *83*(8), 1149–1166.

Ho, S., Tian, L., Disse, M., & Tuo, Y. (2021). A new approach to quantify propagation time from meteorological to hydrological drought. *Journal of Hydrology*, *603*, 127056.

Huang, S., Zhang, X., Chen, N., Li, B., Ma, H., Xu, L., Li, R., & Niyogi, D. (2021). Drought propagation modification after the construction of the Three Gorges Dam in the Yangtze River Basin. *Journal of Hydrology*, *603*, 127138.

Hwang, K., & Cho, S. A. (2007). Constrained learning method based on ontology of Bayesian networks for effective recognition of uncertain scenes. *Journal of KISS: Software and Applications*, *34*(6), 549–561.

Jain, S. K., Shilpa, L. S., Rani, D., & Sudheer, K. P. (2023). State-of-the-art review: Operation of multi-purpose reservoirs during flood season. *Journal of Hydrology*, *618*, 129165.

Jehanzaib, M., Shah, S. A., Yoo, J., & Kim, T.-W. (2020). Investigating the impacts of climate change and human activities on hydrological drought using non-stationary approaches. *Journal of Hydrology*, *588*, 125052.

Jiang, S., Wang, M., Ren, L., Xu, C.-Y., Yuan, F., Liu, Y., Lu, Y., & Shen, H. (2019). A framework for quantifying the impacts of climate change and human activities on hydrological drought in a semiarid basin of Northern China. *Hydrological Processes*, *33*(7), 1075–1088.

Jiang, T., Su, X., Qu, Y., Singh, V. P., Zhang, T., Chu, J., & Hu, X. (2024). Determining the response of ecological drought to meteorological and groundwater droughts in Northwest China using a spatio-temporal matching method. *Journal of Hydrology*, *633*, 130753.

Jin, H., Willems, P., Chen, X., & Liu, M. (2024). Comprehensive evaluation of extreme hydrometeorological events coincidence and their interrelationships in the Hanjiang River Basin, China. *Journal of Hydrology*, *638*, 131506.

van Langen, S. C. H., Costa, A. C., Ribeiro Neto, G. G., & van Oel, P. R. (2021). Effect of a reservoir network on drought propagation in a semi-arid catchment in brazil. *Hydrological Sciences Journal*, *66*(10), 1567–1583.

Leitman, S., Pine, W. E., & Kiker, G. (2016). Management options during the 2011–2012 drought on the Apalachicola River: A systems dynamic model evaluation. *Environmental Management*, *58*(2), 193–207.

Li, C., Qu, Y., Jiang, T., Jiang, F., Wang, Q., Zhang, X., & Xu, X. (2024). Attribution analysis of hydrological drought after the impoundment of the Danjiangkou reservoir in the Hanjiang River Basin. *Journal of Hydrology: Regional Studies*, *56*, 102038.

Li, P., Huang, Q., Huang, S., Leng, G., Peng, J., Wang, H., Zheng, X., Li, Y., & Fang, W. (2022). Various maize yield losses and their dynamics triggered by drought thresholds based on Copula-Bayesian conditional probabilities. *Agricultural Water Management*, *261*, 107391.

Li, R., Chen, N., Zhang, X., Zeng, L., Wang, X., Tang, S., Li, D., & Niyogi, D. (2020). Quantitative analysis of agricultural drought propagation process in the Yangtze River Basin by using cross wavelet analysis and spatial autocorrelation. *Agricultural and Forest Meteorology*, *280*, 107809.

Lin, Q., Wu, Z., Singh, V. P., Sadeghi, S. H. R., He, H., & Lu, G. (2017). Correlation between hydrological drought, climatic factors, reservoir operation, and vegetation cover in the Xijiang Basin, South China. *Journal of Hydrology*, *549*, 512–524.

Liu, H., Wu, J., & Xu, Y. (2018). Investigating the effects of precipitation on drought in the Hanjiang River Basin using SPI. *Journal of Water and Climate Change*, *10*(4), 977–992.

Liu, Q., Yang, Y., Liang, L., Jun, H., Yan, D., Wang, X., Li, C., & Sun, T. (2023a). Thresholds for triggering the propagation of meteorological drought to hydrological drought in water-limited regions of China. *Science of the Total Environment*, *876*, 162771.

Liu, Q., Yang, Y., Liang, L., Yan, D., Wang, X., Li, C., & Sun, T. (2023b). Shift in precipitation-streamflow relationship induced by multi-year drought across global catchments. *Science of the Total Environment*, *857*, 159560.

Liu, X., Luo, Y., Yang, T., Liang, K., Zhang, M., & Liu, C. (2015). Investigation of the probability of concurrent drought events between the water source and destination regions of China's water diversion project: DROUGHT OF CHINA'S WATER DIVERSION. *Geophysical Research Letters*, *42*(20), 8424–8431.

Liu, Y., Shan, F., Yue, H., Wang, X., & Fan, Y. (2023c). Global analysis of the correlation and propagation among meteorological, agricultural, surface water, and groundwater droughts. *Journal of Environmental Management*, *333*, 117460.

Van Loon, A. F. (2015). Hydrological drought explained. *WIREs Water*, *2*(4), 359–392.

Van Loon, A. F., Gleeson, T., Clark, J., Van Dijk, A. I. J. M., Stahl, K., Hannaford, J., Di Baldassarre, G., Teuling, A. J., Tallaksen, L. M., Uijlenhoet, R., Hannah, D. M., Sheffield, J., Svoboda, M., Verbeiren, B., Wagener, T., Rangecroft, S., Wanders, N., & Van Lanen, H. A. J. (2016). Drought in the Anthropocene. *Nature Geoscience*, *9*(2), 89–91.

Van Loon, A. F., & Laaha, G. (2015). Hydrological drought severity explained by climate and catchment characteristics. *Journal of Hydrology*, *526*, 3–14.

Lu, X., Zhuang, Y., Wang, X., & Yang, Q. (2018). Assessment of streamflow change in middle-lower reaches of the Hanjiang River. *Journal of Hydrologic Engineering*, *23*(12), 05018024.

Ma, M., Song, S., Ren, L., Jiang, S., & Song, J. (2013). Multivariate drought characteristics using trivariate Gaussian and student t copulas. *Hydrological Processes*, *27*(8), 1175–1190.

Madadgar, S., & Moradkhani, H. (2014). Spatio-temporal drought forecasting within Bayesian networks. *Journal of Hydrology*, *512*, 134–146.

Miao, C., & Gou, J. (2022). CNRDv1.0: The China natural runoff dataset version 1.0 (1961–2018). National Tibetan Plateau/Third Pole Environment Data Center. https://doi.org/10.11888/Atmos.tpdc.272864

Mtibaa, S., & Asano, S. (2022). Hydrological evaluation of radar and satellite gauge-merged precipitation datasets using the SWAT model: Case of the Terauchi catchment in Japan. *Journal of Hydrology: Regional Studies*, *42*, 101134.

Narasimhan, B., & Srinivasan, R. (2005). Development and evaluation of Soil Moisture Deficit Index (SMDI) and Evapotranspiration Deficit Index (ETDI) for agricultural drought monitoring. *Agricultural and Forest Meteorology*, *133*(1–4), 69–88.

Ouyang, S. Z., Zhong, L., & Luo, R. Q. (2018). The comparison and analysis of extracting video key frame. *IOP Conference Series: Materials Science and Engineering*, *359*, 012010.

Pachore, A., Agrawal, N., Omonov, N., Rakhmonov, K., Umirzakov, G., Mujumdar, S., & Remesan, R. (2024). Evaluation of the impact of anthropogenic storage on the hydrological drought propagation in two contrasting semi-arid river basins. *Journal of Water and Climate Change*, *15*(7), 3276–3292.

Poonia, V., Jha, S., & Goyal, M. K. (2021). Copula based analysis of meteorological, hydrological and agricultural drought characteristics across Indian river basins. *International Journal of Climatology*, *41*(9), 4637–4652.

Prasanchum, H., Tumma, N., & Lohpaisankrit, W. (2022). Establishing spatial distributions of drought phenomena on cultivation seasons using the SWAT model. *Geographia Technica*, *17*(2/2022), 1–13.

Raposo, V. M. B., Costa, V. A. F., & Rodrigues, A. F. (2023). A review of recent developments on drought characterization, propagation, and influential factors. *Science of the Total Environment*, *898*, 165550.

Romeo, J. S., Tanaka, N. I., & Pedroso-De-Lima, A. C. (2006). Bivariate survival modeling: a Bayesian approach based on Copulas. *Lifetime Data Analysis*, *12*(2), 205–222.

Sattar, M. N., Lee, J.-Y., Shin, J.-Y., & Kim, T.-W. (2019). Probabilistic characteristics of drought propagation from meteorological to hydrological drought in South Korea. *Water Resources Management*, *33*(7), 2439–2452.

Senbeta, T. B., Napiórkowski, J. J., Karamuz, E., Kochanek, K., & Woyessa, Y. E. (2024). Impacts of water regulation through a reservoir on drought dynamics and propagation in the Pilica River watershed. *Journal of Hydrology: Regional Studies*, *53*, 101812.

Shao, J. (1997). An asymptotic theory for linear model selection. *Statistica Sinica*, *7*(2), 221–264.

Shiau, J.-T. (2023). Causality-based drought propagation analyses among meteorological drought, hydrologic drought, and water shortage. *Science of the Total Environment*, *888*, 164216.

Sreeparvathy, V., & Srinivas, V. V. (2022). Meteorological flash droughts risk projections based on CMIP6 climate change scenarios. *npj Climate and Atmospheric Science*, *5*(1), 77.

Vicente-Serrano, S. M., Beguería, S., & López-Moreno, J. I. (2010). A multiscalar drought index sensitive to global warming: The standardized precipitation evapotranspiration index. *Journal of Climate*, *23*(7), 1696–1718.

Vicente-Serrano, S. M., López-Moreno, J. I., Beguería, S., Lorenzo-Lacruz, J., Azorin-Molina, C., & Morán-Tejeda, E. (2012). Accurate computation of a streamflow drought index. *Journal of Hydrologic Engineering*, *17*(2), 318–332.

Van de Vyver, H., & Van den Bergh, J. (2018). The Gaussian copula model for the joint deficit index for droughts. *Journal of Hydrology*, *561*, 987–999.

Wang, F., Lai, H., Li, Y., Feng, K., Zhang, Z., Tian, Q., Zhu, X., & Yang, H. (2022a). Dynamic variation of meteorological drought and its relationships with agricultural drought across China. *Agricultural Water Management*, *261*, 107301.

Wang, H., Wang, Z., Bai, Y., & Wang, W. (2024). Propagation characteristics of meteorological drought to hydrological drought considering nonlinear correlations - A case study of the Hanjiang River Basin, China. *Ecological Informatics*, *80*, 102512.

Wang, L., Zhang, J., Elmahdi, A., Shu, Z., Wu, Y., & Wang, G. (2021). Evolution characteristics and relationship of meteorological and hydrological droughts from 1961 to 2018 in Hanjiang River Basin, China. *Journal of Water and Climate Change*, *13*(1), 224–246.

Wang, Y., Li, J., Zhang, T., & Wang, B. (2019). Changes in drought propagation under the regulation of reservoirs and water diversion. *Theoretical and Applied Climatology*, *138*(1–2), 701–711.

Wang, Y., Peng, T., He, Y., Singh, V. P., Lin, Q., Dong, X., Fan, T., Liu, J., Guo, J., & Wang, G. (2023a). Attribution analysis of non-stationary hydrological drought using the GAMLSS framework and an improved SWAT model. *Journal of Hydrology*, *627*, 130420.

Wang, Y., Peng, T., Lin, Q., Singh, V. P., Dong, X., Chen, C., Liu, J., Chang, W., & Wang, G. (2022b). A new non-stationary hydrological drought index encompassing climate indices and modified reservoir index as covariates. *Water Resources Management*, *36*(7), 2433–2454.

Wang, Y., Wang, D., & Wu, J. (2015). Assessing the impact of Danjiangkou reservoir on ecohydrological conditions in Hanjiang river, China. *Ecological Engineering*, *81*, 41–52.

Wang, Y. X., Peng, T., He, Y. H., Singh, V. P., Lin, Q. X., Dong, X. H., Fan, T. Y., Liu, J., Guo, J. L., & Wang, G. X. (2023b). Attribution analysis of non-stationary hydrological drought using the GAMLSS framework and an improved SWAT model. *Journal of Hydrology*, *627*, 130420.

Wen, L., Rogers, K., Ling, J., & Saintilan, N. (2011). The impacts of river regulation and water diversion on the hydrological drought characteristics in the Lower Murrumbidgee River, Australia. *Journal of Hydrology*, *405*(3–4), 382–391.

Wen, W., Jingshu, W., Yiyuan, T., & Hui, C. (2020). Research progress on the impact of human activities on the formation and development of hydrological drought. *Journal of China Hydrology*, *40*(3), 1–8.

Wilhite, D. A., & Glantz, M. H. (1985). Understanding: the drought phenomenon: The role of definitions. *Water International*, *10*(3), 111–120.

Wu, H., Su, X., Singh, V. P., AghaKouchak, A., & Liu, Z. (2023). Bayesian vine copulas improve agricultural drought prediction for long lead times. *Agricultural and Forest Meteorology*, *331*, 109326.

Wu, J., Chen, X., Gao, L., Yao, H., Chen, Y., & Liu, M. (2016). Response of hydrological drought to meteorological drought under the influence of large reservoir. *Advances in Meteorology*, *2016*, 1–11.

Wu, J., Chen, X., Yao, H., Gao, L., Chen, Y., & Liu, M. (2017). Nonlinear relationship of hydrological drought responding to meteorological drought and impact of a large reservoir. *Journal of Hydrology*, *551*, 495–507.

Wu, J., Chen, X., Yao, H., & Zhang, D. (2021a). Multi-timescale assessment of propagation thresholds from meteorological to hydrological drought. *Science of the Total Environment*, *765*, 144232.

Wu, J., Liu, Z., Yao, H., Chen, X., Chen, X., Zheng, Y., & He, Y. (2018). Impacts of reservoir operations on multi-scale correlations between hydrological drought and meteorological drought. *Journal of Hydrology*, *563*, 726–736.

Wu, J., Yao, H., Chen, X., Wang, G., Bai, X., & Zhang, D. (2022). A framework for assessing compound drought events from a drought propagation perspective. *Journal of Hydrology*, *604*, 127228.

Wu, J., Yuan, X., Yao, H., Chen, X., & Wang, G. (2021b). Reservoirs regulate the relationship between hydrological drought recovery water and drought characteristics. *Journal of Hydrology*, *603*, 127127.

Wu, J., Zhang, X., Wang, G., Wu, W., Zhang, D., & Lan, T. (2024). Impacts of hydrometeorological regime shifts on drought propagation: The meteorological to hydrological perspective. *Journal of Hydrology*, *638*, 131476.

Xing, Z., Ma, M., Zhang, X., Leng, G., Su, Z., Lv, J., Yu, Z., & Yi, P. (2021). Altered drought propagation under the influence of reservoir regulation. *Journal of Hydrology*, *603*, 127049.

Xu, Y., Zhang, X., Wang, X., Hao, Z., Singh, V. P., & Hao, F. (2019). Propagation from meteorological drought to hydrological drought under the impact of human activities: A case study in northern China. *Journal of Hydrology*, *579*, 124147.

Xu, Z., Wu, Z., Shao, Q., He, H., & Guo, X. (2023). From meteorological to agricultural drought: Propagation time and probabilistic linkages. *Journal of Hydrology: Regional Studies*, *46*, 101329.

Yang, X., Wu, F., Yuan, S., Ren, L., Sheffield, J., Fang, X., Jiang, S., & Liu, Y. (2024). Quantifying the impact of human activities on hydrological drought and drought propagation in China using the PCR-GLOBWB v2.0 model. *Water Resources Research*, *60*(1), e2023WR035443.

Ye, X., Li, X., Xu, C.-Y., & Zhang, Q. (2016). Similarity, difference and correlation of meteorological and hydrological drought indices in a humid climate region – the Poyang Lake catchment in China. *Hydrology Research*, *47*(6), 1211–1223.

Yevjevich, V. M. (1967). An objective approach to definitions and investigations of continental hydrologic droughts. *Journal of Hydrology*, *7*(3), 353.

Yuan, X., Zhang, M., Wang, L., & Zhou, T. (2017). Understanding and seasonal forecasting of hydrological drought in the Anthropocene. *Hydrology and Earth System Sciences*, *21*(11), 5477–5492.

Zhang, D., Zhang, Q., Qiu, J., Bai, P., Liang, K., & Li, X. (2018). Intensification of hydrological drought due to human activity in the middle reaches of the Yangtze River, China. *Science of the Total Environment*, *637–638*, 1432–1442.

Zhang, Q., Miao, C., Guo, X., Gou, J., & Su, T. (2023a). Human activities impact the propagation from meteorological to hydrological drought in the Yellow River Basin, China. *Journal of Hydrology*, *623*, 129752.

Zhang, T., Su, X., & Wu, L. (2023). Integrating multiple comparison methods for attributing hydrological drought evolution and drought propagation: The impact of climate change cannot be ignored. *Journal of Hydrology*, *621*, 129557.

Zhang, X., Hao, Z., Singh, V. P., Zhang, Y., Feng, S., Xu, Y., & Hao, F. (2022). Drought propagation under global warming: Characteristics, approaches, processes, and controlling factors. *Science of the Total Environment*, *838*(2), 156021.

Zhang, X., Ren, G., Bing, H., Mikami, T., Matsumoto, J., Zhang, P., & Yang, G. (2023b). Reconstruction and characterization of droughts and floods in the Hanjiang River Basin, China, 1426–2017. *Climatic Change*, *176*(5), 62.

Zhang, X., She, D., Xia, J., Zhang, L., Deng, C., & Liu, Z. (2023). The changing characteristics of propagation time from meteorological drought to hydrological drought in the Yangtze River Basin, China. *Atmospheric Research*, *290*, 106774.

Zhao, M., Huang, S., Huang, Q., Wang, H., Leng, G., & Xie, Y. (2019). Assessing socio-economic drought evolution characteristics and their possible meteorological driving force. *Geomatics, Natural Hazards and Risk*, *10*(1), 1084–1101.

Zhou, M., Xiong, L., Jiang, C., Chen, G., Liu, C., & Zha, X. (2024). River network-based index to clarify transmission of hydrological drought in reservoir-regulated basins. *Journal of Hydrology: Regional Studies*, *51*, 101604.

Zhou, Z., Shi, H., Fu, Q., Ding, Y., Li, T., Wang, Y., & Liu, S. (2021). Characteristics of propagation from meteorological drought to hydrological drought in the Pearl River Basin. *Journal of Geophysical Research: Atmospheres*, *126*(4), e2020JD033959.

Zhou, Z., Wang, P., Li, L., Fu, Q., Ding, Y., Chen, P., Xue, P., Wang, T., & Shi, H. (2024). Recent development on drought propagation: A comprehensive review. *Journal of Hydrology*, *645*(B), 132196.

Zhu, Z., Duan, W., Zou, S., Zeng, Z., Chen, Y., Feng, M., Qin, J., & Liu, Y. (2024). Spatiotemporal characteristics of meteorological drought events in 34 major global river basins during 1901–2021. *Science of the Total Environment*, *921*, 170913.

How to cite this article: Qu, Y., Li, C., Zhang, Y., Zhao, S., Jiang, T., & Ye, Q. (2026). Study of meteorological-hydrological drought propagation under reservoir regulation using a Copula-Bayesian network in the Hanjiang River Basin. *River*, *5*, 33–54. https://doi.org/10.1002/rvr2.70045